

On the possibility of testing the two-peak structure of the LHCb hidden-charm strange pentaquark $P_{cs}(4459)^0$ in near-threshold antikaon-induced charmonium production on protons and nuclei

E. Ya. Paryev

*Institute for Nuclear Research of the Russian Academy of Sciences
Moscow, Russia*

Abstract

Accounting for the LHCb observation that the reported hidden-charm strange pentaquark $P_{cs}(4459)^0$ can split into two substructures, $P_{cs}(4455)^0$ and $P_{cs}(4468)^0$, with a mass difference of 13 MeV as well as the newly observed hidden-charm pentaquark resonance $P_{cs}(4338)^0$ with strangeness, we study within the double-peak scenario for the $P_{cs}(4459)^0$ state the near-threshold J/ψ meson production from protons and nuclei by considering incoherent direct non-resonant ($K^-p \rightarrow J/\psi\Lambda$) and two-step resonant ($K^-p \rightarrow P_{csi}^0 \rightarrow J/\psi\Lambda$, $i = 1, 2, 3$; $P_{cs1}^0 = P_{cs}(4338)^0$, $P_{cs2}^0 = P_{cs}(4455)^0$, $P_{cs3}^0 = P_{cs}(4468)^0$) charmonium production processes with the main goal of clarifying the possibility to observe within this scenario both above two substructures contributing to the $P_{cs}(4459)^0$ state and the $P_{cs}(4338)^0$ resonance in this production. We calculate the absolute excitation functions, energy and momentum distributions for the non-resonant, resonant and for the combined (non-resonant plus resonant) production of J/ψ mesons on protons as well as on carbon and tungsten target nuclei at near-threshold incident antikaon beam momenta by assuming the spin-parity assignments of the hidden-charm resonances $P_{cs}(4338)^0$, $P_{cs}(4455)^0$ and $P_{cs}(4468)^0$ as $J^P = (1/2)^-$, $J^P = (1/2)^-$ and $J^P = (3/2)^-$ within four different realistic choices for the branching ratios of their decays to the $J/\psi\Lambda$ mode (0.125, 0.25, 0.5 and 1%) as well as for two options for the branching fraction of their decays to the K^-p channel (0.01 and 0.001%). We show that these combined observables reveal clear sensitivity to these scenarios. Hence, they may be an important tool to provide further evidence for the existence of the above strange hidden-charm pentaquark resonances.

1. Introduction

The study of pentaquark states, comprising four quarks and an antiquark, has received considerable interest in recent years. The first observation of the hidden-charm pentaquark resonances $P_c(4380)^+$ and $P_c(4450)^+$ in the $J/\psi p$ invariant mass spectrum of the $\Lambda_b^0 \rightarrow K^-(J/\psi p)$ decays has been reported by the LHCb experiment [1]¹⁾. With the inclusion of additional data, it was found that the $P_c(4450)^+$ state is composed of two narrow overlapping peaks, $P_c(4440)^+$ and $P_c(4457)^+$. In addition, a new narrow state, the $P_c(4312)^+$ was discovered [3]. Recently, evidence for a new narrow hidden-charm pentaquark denoted as $P_c(4337)^+$ was found in the invariant mass spectrum of the $J/\psi p$ in the $B_s^0 \rightarrow J/\psi p \bar{p}$ decays [4]. The minimal quark structure of the above pentaquarks is $|P_c^+ \rangle = |uudc\bar{c} \rangle$. In a molecular scenario, due to the closeness of the observed $P_c(4312)^+$ and $P_c(4440)^+$, $P_c(4457)^+$ masses to the $\Sigma_c^+ \bar{D}^0$ and $\Sigma_c^+ \bar{D}^{*0}$ thresholds, the $P_c(4312)^+$ resonance can be, in particular, interpreted as an S-wave $\Sigma_c^+ \bar{D}^0$ bound state, while the $P_c(4440)^+$ and $P_c(4457)^+$ as S-wave $\Sigma_c^+ \bar{D}^{*0}$ bound molecular states [5–16], though their inner structure (charmed baryon–charmed antimeson two-body molecule or compact pentaquark state) is still not determined and there are alternative explanations too [17–20]. Due to lacking nearby meson-baryon thresholds, the $P_c(4337)^+$ is difficult to accommodate within the molecular picture [21, 22]. But, it is more natural to view it as the compact pentaquark state [19, 23]. The LHCb Collaboration announced recently also the discovery of two new narrow hidden-charm strange pentaquark states, $P_{cs}(4459)^0$ [24] and $P_{cs}(4338)^0$ [25], with minimal quark content $|udsc\bar{c} \rangle$ in the invariant mass spectra of the $J/\psi \Lambda$ in the $\bar{b}^- \rightarrow K^-(J/\psi \Lambda)$ and $B^- \rightarrow \bar{p}(J/\psi \Lambda)$ decays²⁾. The Breit-Wigner masses and total widths of these exotic states were measured to be [24, 25]:

$$P_{cs}(4459)^0 : M = 4458.8 \pm 2.9_{-1.1}^{+4.7} \text{ MeV}, \quad \Gamma = 17.3 \pm 6.5_{-5.7}^{+8.0} \text{ MeV}; \quad (1)$$

$$P_{cs}(4338)^0 : M = 4338.2 \pm 0.7 \pm 0.4 \text{ MeV}, \quad \Gamma = 7.0 \pm 1.2 \pm 1.3 \text{ MeV}. \quad (2)$$

While the spin-parity quantum numbers J^P of the $P_{cs}(4459)^0$ resonance were not experimentally determined due to a limited signal yield, the spin of the $P_{cs}(4338)^0$ pentaquark candidate is determined to be $J = 1/2$ and negative parity is preferred [25]. Since the new strange $P_{cs}(4459)^0$ and $P_{cs}(4338)^0$ pentaquarks are found close to thresholds for the production of ordinary baryon-meson states $\Xi_c \bar{D}^*$ and $\Xi_c \bar{D}$ ³⁾, it is natural to interpret them as the hidden-charm singly-strange $\Xi_c \bar{D}^*$ and $\Xi_c \bar{D}$ molecules. Such plausible molecular interpretation of the $P_{cs}(4459)^0$ and $P_{cs}(4338)^0$ exotic states with strangeness was supported by many current theoretical studies (see, e.g., Refs. [23–38]) and is commonly accepted. However, there exists another explanations of the P_{cs} states, based both on the compact quark model [19, 39–42] and on other molecular picture [43], in which it was found that due to the extra attraction obtained in the $\Xi_c \bar{D}^*$, $\Xi_c \bar{D}$ pairs the $P_{cs}(4459)^0$ and $P_{cs}(4338)^0$ states are associated, respectively, to the $\Xi_c' \bar{D}$ and $\Xi_c \bar{D}^*$. It should be pointed out that the existence of hidden-charm strange pentaquark resonances P_{cs} has been predicted before the LHCb experiment [24] in some earlier papers (see, for example, Refs. [15, 44–53]). It is also worth noting that the large Q -values of the decays $P_{cs}(4459)^0 \rightarrow J/\psi \Lambda$ and $P_{cs}(4338)^0 \rightarrow J/\psi \Lambda$ (in which the pentaquarks $P_{cs}(4459)^0$ and $P_{cs}(4338)^0$ were observed) – respectively, 246 MeV and 126 MeV – and unnaturally small for such Q -values widths of the $P_{cs}(4459)^0$ and $P_{cs}(4338)^0$ states about of 17 MeV and 7 MeV tell us in favor of $\Xi_c \bar{D}^*$ and $\Xi_c \bar{D}$ molecular interpretation of these states since in this interpretation their decay into the $J/\psi \Lambda$ is naturally suppressed due to the fact that two c

¹⁾For better readability of this paper, the old exotic hadron naming scheme is used throughout it instead of the new one proposed in Ref. [2]. According to the latter one, the P_ψ^N would be the new name for the P_c states.

²⁾Following the new naming convention in [2], in Ref. [25] these newly observed states are named as $P_{\psi s}^\Lambda(4459)^0$ and $P_{\psi s}^\Lambda(4338)^0$.

³⁾The pole mass of the $P_{cs}(4459)^0$ state is just about 19 MeV below the $\Xi_c^0 \bar{D}^{*0}$ threshold [24]. The central value of the $P_{cs}(4338)^0$ mass is only 0.8 and 2.9 MeV above, respectively, the $\Xi_c^+ D^-$ and $\Xi_c^0 \bar{D}^0$ thresholds [26].

and \bar{c} quarks, belonging, respectively, to the Ξ_c baryon and \bar{D}^* , \bar{D} mesons, in hadronic molecules are well-separated and it is unlikely for them to be close to each other to form a single J/ψ meson, which provides decay-suppressing mechanism [26, 29]. Along the way of molecular scenario for the $P_{cs}(4459)^0$ resonance, one can easily find its possible spin-parity quantum numbers. Considering it as pure $\Xi_c\bar{D}^*$ molecule, in which Ξ_c baryon with $J^P = (1/2)^+$ and antimeson \bar{D}^* with $J^P = (1)^-$ are in a relative S-wave, we get that the spin-parity of the $P_{cs}(4459)^0$ is either $J^P = (1/2)^-$ or $J^P = (3/2)^-$ (cf. Ref. [26])⁴. This conclusion was supported by more elaborate theoretical approaches (see, e.g., Refs. [19, 30, 34, 36, 37, 39, 40, 41, 48, 54]), in which the $P_{cs}(4459)^0$ is considered as $\Xi_c\bar{D}^*$ molecular pentaquark state [30, 34, 36, 37, 48, 54] or as compact pentaquark state [19, 39, 40, 41]. In the absence of coupled-channel effects the heavy-quark spin symmetry predicts the two $\Xi_c\bar{D}^*$ states (with total spin $J = 1/2$ and $J = 3/2$, respectively) to be degenerate [55]. Their inclusion breaks the spin degeneracy of the $P_{cs}(4459)^0$ and generates a hyperfine splitting between the two spin configurations [21, 27, 31, 32, 33, 35, 38, 50, 55, 56], in which the $J^P = (1/2)^-$ $\Xi_c\bar{D}^*$ pentaquark will be lighter than the $J^P = (3/2)^-$ one [27, 38, 50] and vice versa [21, 31, 32, 33, 35, 55, 56]. This means that in the mass region of the $P_{cs}(4459)^0$ (slightly below the $\Xi_c\bar{D}^*$ threshold) may exist two almost degenerate narrow overlapping $\Xi_c\bar{D}^*$ molecular states, similar to the case for the non-strange hidden-charm pentaquark $P_c(4450)^+$, which can be equally replaced by two pentaquark substructures $P_c(4440)^+$ and $P_c(4457)^+$ [3]. In particular, in this region Ref. [50] predicts, within the chiral effective field theory, the masses of the two $\Xi_c\bar{D}^*$ molecular states to be:

$$\begin{aligned}\Xi_c\bar{D}^* \text{ with } J^P = (1/2)^- : M &= 4456.9_{-3.3}^{+3.2} \text{ MeV}, \\ \Xi_c\bar{D}^* \text{ with } J^P = (3/2)^- : M &= 4463.0_{-3.0}^{+2.8} \text{ MeV}.\end{aligned}\tag{3}$$

Motivated by these findings, the LHCb Collaboration tested the hypothesis of the two-peak structure of the $P_{cs}(4459)^0$ resonance [24] with the predicted in [50] J^P values. It was found [24] that this resonance can also well be described by two pentaquark resonances with mass difference of 13 MeV, named in the present paper as $P_{cs}(4455)^0$ and $P_{cs}(4468)^0$ (cf. [21, 26]). Their masses and widths were determined to be:

$$\begin{aligned}P_{cs}(4455)^0 : M &= 4454.9 \pm 2.7 \text{ MeV}, \quad \Gamma = 7.5 \pm 9.7 \text{ MeV}; \\ P_{cs}(4468)^0 : M &= 4467.8 \pm 3.7 \text{ MeV}, \quad \Gamma = 5.2 \pm 5.3 \text{ MeV}.\end{aligned}\tag{4}$$

We see that the 'experimental' masses (4) are in excellent agreement with the calculated ones of Eq. (3). This fact and the theoretical predictions of the double-peak structure of the $\Xi_c\bar{D}^*$ molecule in the energy region of the $P_{cs}(4459)^0$ resonance, discussed above, make us suggest that the $P_{cs}(4459)^0$ should indeed contain two substructures. And from now on, we will assume the existence of the two $P_{cs}(4455)^0$ and $P_{cs}(4468)^0$ peaks in spite of the fact that the LHCb analysis of the current data sample cannot confirm or disprove the two-peak solution (4). One may hope that the future more precise LHCb measurements and other ones, stimulated, in particular, by the results of the present work, would indeed shed light on whether the double-peak interpretation of the $P_{cs}(4459)^0$ state is correct.

Remarkably, another hidden-charm exotic state with open strangeness – the strange hidden-charm tetraquark state $Z_{cs}(3985)^-$, decaying into $D_s^- D^{*0}$ and $D_s^{*-} D^0$, has been observed in 2020 by the BESIII Collaboration in the processes $e^+e^- \rightarrow K^+(D_s^- D^{*0} + D_s^{*-} D^0)$ [57]. This state has the minimal quark content $Z_{cs}(3985)^- = |\bar{u}sc\bar{c}\rangle$. It is in the proximity of the $D_s^- D^{*0}/D_s^{*-} D^0$ mass thresholds and can be interpreted [58, 59] as strange molecular partner with hadronic molecular configuration $D_s^- D^{*0} - D_s^{*-} D^0$ of the non-strange tetraquark resonance $Z_c(3900)^-$, having the valence

⁴Similarly, identifying the $P_{cs}(4338)^0$ state as the S-wave $\Xi_c(1/2)^+\bar{D}(0^-)$ molecular state, we obtain that its spin-parity combination would be $J^P = (1/2)^-$ – what exactly was observed in the LHCb experiment [25].

quark content $Z_c(3900)^- = |\bar{u}dc\bar{c}\rangle$ and possible hadronic molecular structure $D^-D^{*0} - D^{*-}D^0$. Moreover, in 2022 year the BESIII Collaboration reported [60] evidence for the neutral $Z_{cs}(3985)^0$ state in the processes $e^+e^- \rightarrow K_S^0(D_s^+D^{*-} + D_s^{*+}D^-)$, whose mass and width are close to those of the charged $Z_{cs}(3985)^-$. Hence, the $Z_{cs}(3985)^0$ can be regarded as the isospin partner of the $Z_{cs}(3985)^-$. Earlier, the LHCb Collaboration reported the first observation of exotic states $Z_{cs}(4000)^+$ and $Z_{cs}(4220)^+$ with a new quark content $|u\bar{s}c\bar{c}\rangle$ in the mass spectra of the $J/\psi K^+$ in $B^+ \rightarrow J/\psi\phi K^+$ decays [61]. Furthermore, the first results of searching for a heavier partner of the observed $Z_{cs}(3985)^-$ state, denoted as $Z_{cs}'^-$, in the process $e^+e^- \rightarrow K^+D_s^{*-}D^{*0}$ (c.c.) with the BESIII detector have been reported in very recent publication [62]. In addition, one needs to note that possible hidden-charm pentaquarks, having two and three strange quarks in their valence composition (or pentaquarks with double and triple strangeness), have been theoretically investigated in Refs. [19, 49, 63, 64, 65, 66]. They are at present an experimentally virgin territory. But one may hope that they will be discovered in the foreseeable future at the LHC as well. It should be noticed that the investigation of magnetic moments of the hidden-charm pentaquark states without strangeness, with strangeness and with double strangeness, which play an important role in understanding their internal structure, has been performed, in particular, in Ref. [67] within the QCD light-cone sum rules. Extensive reviews of the recent experimental and theoretical progresses in the field of heavy hadronic molecular states are presented in Refs. [18, 68].

Confirming the $P_{cs}(4459)^0$ and $P_{cs}(4338)^0$ states, observed in the Ξ_b^- and B^- decays at LHCb, in other processes would provide independent and complementary verification of their existence as well as would be helpful both to understand their nature and to pin down their resonance parameters. In that way, the production of the single-peak $P_{cs}(4459)^0$ pentaquark in antikaon-induced and photon-induced reactions on nuclear targets was discussed in Refs. [69, 70] and [71], correspondingly. In fact, in Ref. [69] the contribution of this pentaquark to the elementary $K^-p \rightarrow J/\psi\Lambda$ reaction has been determined, employing two different theoretical approaches, i.e., the effective Lagrangian and the Regge models. It was shown that the $P_{cs}(4459)^0$ can also be searched for through a scan of the total and differential cross sections of this reaction. In our work [70], we have calculated the absolute excitation functions, energy and momentum distributions for the direct non-resonant ($K^-p \rightarrow J/\psi\Lambda$), two-step resonant ($K^-p \rightarrow P_{cs}(4459)^0 \rightarrow J/\psi\Lambda$) and for the combined (non-resonant plus resonant) production of J/ψ mesons off protons as well as off carbon and tungsten target nuclei at near-threshold incident antikaon energies by assuming the spin-parity assignment of the $P_{cs}(4459)^0$ resonance as $J^P = (3/2)^-$ within six different scenarios for the branching ratio $Br[P_{cs}(4459)^0 \rightarrow J/\psi\Lambda]$ of the decay $P_{cs}(4459)^0 \rightarrow J/\psi\Lambda$, namely: $Br[P_{cs}(4459)^0 \rightarrow J/\psi\Lambda] = 1, 3, 5, 10, 15$ and 50% . We also have shown that the combined observables considered reveal definite sensitivity to these scenarios, which means that they may be an important tool to provide further evidence for the existence of the pentaquark $P_{cs}(4459)^0$ resonance and to get valuable information on its decay rate to the $J/\psi\Lambda$ final state. It should be noted that the energy of the negative kaon beam, which will be available at the K10 beam line in the extended J-PARC Hadron Experimental Facility [72], will be sufficient to observe the $P_{cs}(4459)^0$ pentaquark via the $K^-p \rightarrow J/\psi\Lambda$ process. The possibility of searching for this pentaquark in $\gamma p \rightarrow K^+P_{cs}(4459)^0$ reaction, assuming that it with the spin-parity combinations $J^P = (1/2)^-$ or $J^P = (3/2)^-$ can be interpreted as a $\Xi_c\bar{D}^*$ molecule or as a compact pentaquark, has been investigated in Ref. [71]. It was shown that the total cross section of this reaction, calculated in the latter picture of the $P_{cs}(4459)^0$, is quite different from that, obtained in molecular scenario of the $P_{cs}(4459)^0$, which can be used to test the nature of the $P_{cs}(4459)^0$ state [71]. And finally, in the recent work [73], based on the hadronic molecular picture, the authors have estimated the semi-inclusive electroproduction rates, in particular, of the $P_{cs}(4459)^0$ and $P_{cs}(4338)^0$ multiquark states at the proposed electron-ion colliders in China (EicC), US (EIC) and at the proposed 24 GeV upgrade of CEBAF.

In the present article, assuming in view of the aforementioned that the $P_{cs}(4459)^0$ resonance splits into two peaks, $P_{cs}(4455)^0$ and $P_{cs}(4468)^0$, with $J^P = (1/2)^-$ and $J^P = (3/2)^-$, respectively,

we consider the contribution both from these peaks and from the $P_{cs}(4338)^0$ state to near-threshold J/ψ meson production by antikaons on protons and nuclei by adopting the standard Breit-Wigner shape for this contribution and by employing an available at present information on the total and differential cross sections of the direct $K^-p \rightarrow J/\psi\Lambda$ process to estimate the background contribution. The main goal of this consideration is also to clarify the possibility of experimental observation of the above two peaks and the $P_{cs}(4338)^0$ state in this production. The consideration is strictly based on the model, developed in Ref. [70]. We briefly recall its main assumptions and describe, where necessary, the corresponding extensions. We present the predictions obtained within this extended model for the J/ψ excitation functions, energy and momentum distributions in K^-p as well as in $K^{-12}\text{C}$ and $K^{-184}\text{W}$ reactions at near-threshold incident antikaon momenta assuming different scenarios for the branching fractions of the decays $P_{cs}(4338/4455/4468)^0 \rightarrow K^-p$ and $P_{cs}(4338/4455/4468)^0 \rightarrow J/\psi\Lambda$. These predictions may serve as guidance for future dedicated experiment at the J-PARC facility devoted to the study of possible two-peak structure of the $P_{cs}(4459)^0$ resonance.

2. Theoretical framework

2.1. Direct non-resonant J/ψ production process

Direct non-resonant charmonium production on nuclear targets in the near-threshold laboratory incident K^- beam momentum region $8.844 \text{ GeV}/c \leq p_{K^-} \leq 10.200 \text{ GeV}/c$ ⁵⁾ may proceed via the following elementary process, which has the lowest free $J/\psi\Lambda$ production threshold momentum (8.844 GeV/c) and in which the strangeness $S = -1$ is conserved [69, 70]:

$$K^- + p \rightarrow J/\psi + \Lambda. \quad (5)$$

Before going further, let us get a feeling about kinematic characteristics of J/ψ mesons – laboratory polar production angles and momenta (total energies), allowed in this process in the simpler case of a free target proton being at rest at an incident resonant antikaon momenta of 9.417, 9.965 and 10.026 GeV/c of our main interest. The kinematics of two-body reaction with a threshold (as in our present case) indicate that the laboratory polar J/ψ production angle $\theta_{J/\psi}$ varies from 0 to a maximal value $\theta_{J/\psi}^{\max}$, i.e.:

$$0 \leq \theta_{J/\psi} \leq \theta_{J/\psi}^{\max}, \quad (6)$$

where

$$\theta_{J/\psi}^{\max} = \arcsin[(\sqrt{s}p_{J/\psi}^*)/(m_{J/\psi}p_{K^-})]. \quad (7)$$

Here, the J/ψ c.m. momentum $p_{J/\psi}^*$ is determined by the equation

$$p_{J/\psi}^* = \frac{1}{2\sqrt{s}}\lambda(s, m_{J/\psi}^2, m_{\Lambda}^2), \quad (8)$$

in which the quantities $m_{J/\psi}$ and m_{Λ} are the free space charmonium and Λ hyperon masses and the vacuum collision energy squared s and function $\lambda(x, y, z)$ are defined, respectively, by the formulas

$$s = (E_{K^-} + m_p)^2 - p_{K^-}^2, \quad E_{K^-} = \sqrt{m_{K^-}^2 + p_{K^-}^2}, \quad (9)$$

⁵⁾In which the pentaquark states $P_{cs}(4338)^0$, $P_{cs}(4455)^0$ and $P_{cs}(4468)^0$ are concentrated and where they can be observed in the K^-p reactions (see Figs. 1 and 2 below). We recall that the threshold (resonant) momenta $p_{K^-}^{\text{R1}}$, $p_{K^-}^{\text{R2}}$ and $p_{K^-}^{\text{R3}}$ for the production of the $P_{cs}(4338)^0$, $P_{cs}(4455)^0$ and $P_{cs}(4468)^0$ resonances with central values of their masses $M_{cs1} = 4338.2$ MeV, $M_{cs2} = 4454.9$ MeV and $M_{cs3} = 4467.8$ MeV (cf. Eqs. (2), (4)) on a free target proton being at rest are $p_{K^-}^{\text{R1}} = 9.417$ GeV/c, $p_{K^-}^{\text{R2}} = 9.965$ GeV/c and $p_{K^-}^{\text{R3}} = 10.026$ GeV/c, respectively.

$$\lambda(x, y, z) = \sqrt{[x - (\sqrt{y} + \sqrt{z})^2][x - (\sqrt{y} - \sqrt{z})^2]}. \quad (10)$$

The quantities m_p and m_{K^-} , entering into Eq. (9), denote the vacuum proton and K^- meson masses. From Eq. (7) one can get that

$$\theta_{J/\psi}^{\max} = 3.932^\circ, \quad \theta_{J/\psi}^{\max} = 5.377^\circ \text{ and } \theta_{J/\psi}^{\max} = 5.507^\circ \quad (11)$$

at initial resonant antikaon beam momenta of 9.417, 9.965 and 10.026 GeV/c, respectively. Energy-momentum conservation in the reaction (5), proceeding on a free target proton at rest, tells us that the kinematically allowed J/ψ meson laboratory momentum $p_{J/\psi}$ and total energy $E_{J/\psi}$ ($E_{J/\psi} = \sqrt{m_{J/\psi}^2 + p_{J/\psi}^2}$) in this reaction vary within the following momentum and energy ranges at given initial antikaon momentum:

$$p_{J/\psi}^{(2)}(0^\circ) \leq p_{J/\psi} \leq p_{J/\psi}^{(1)}(0^\circ), \quad (12)$$

$$E_{J/\psi}^{(2)}(0^\circ) \leq E_{J/\psi} \leq E_{J/\psi}^{(1)}(0^\circ), \quad (13)$$

where the quantities $p_{J/\psi}^{(1,2)}(0^\circ)$ and $E_{J/\psi}^{(1,2)}(0^\circ)$ are the J/ψ momenta and energies at zero polar charmonium production angle in the laboratory frame. They are defined as follows [70]:

$$p_{J/\psi}^{(1,2)}(0^\circ) = \gamma_{\text{cm}} E_{J/\psi}^*(v_{\text{cm}} \pm v_{J/\psi}^*), \quad (14)$$

$$E_{J/\psi}^{(1,2)}(0^\circ) = \gamma_{\text{cm}} (E_{J/\psi}^* \pm v_{\text{cm}} p_{J/\psi}^*). \quad (15)$$

Here,

$$\gamma_{\text{cm}} = (E_{K^-} + m_p)/\sqrt{s}, \quad v_{\text{cm}} = p_{K^-}/(E_{K^-} + m_p), \quad v_{J/\psi}^* = p_{J/\psi}^*/E_{J/\psi}^*, \quad E_{J/\psi}^* = \sqrt{m_{J/\psi}^2 + p_{J/\psi}^{*2}}. \quad (16)$$

The sign "+" in Eqs. (14), (15) corresponds to the first quantities $p_{J/\psi}^{(1)}$, $E_{J/\psi}^{(1)}$ and sign "-" - to the second ones $p_{J/\psi}^{(2)}$, $E_{J/\psi}^{(2)}$. In line with Eqs. (14), (15), for $p_{K^-} = 9.417$ GeV/c the inequalities (12), (13) are:

$$5.695 \leq p_{J/\psi} \leq 7.898 \text{ GeV/c}, \quad (17)$$

$$6.483 \leq E_{J/\psi} \leq 8.484 \text{ GeV}. \quad (18)$$

For $p_{K^-} = 9.965$ GeV/c we obtain:

$$5.488 \leq p_{J/\psi} \leq 8.668 \text{ GeV/c}, \quad (19)$$

$$6.300 \leq E_{J/\psi} \leq 9.205 \text{ GeV}. \quad (20)$$

And for $p_{K^-} = 10.026$ GeV/c we also have:

$$5.471 \leq p_{J/\psi} \leq 8.748 \text{ GeV/c}, \quad (21)$$

$$6.286 \leq E_{J/\psi} \leq 9.280 \text{ GeV}. \quad (22)$$

Obviously, the binding of target protons and their Fermi motion will distort the distributions of the outgoing high-momentum (and high-energy) J/ψ mesons ⁶⁾ as well as lead to a wider accessible momentum and energy intervals compared to those given above by Eqs. (17)–(22). With this, we will ignore the modification of the final high-momentum J/ψ meson and Λ hyperon in the nuclear medium in the present work in the case when the reaction $K^-p \rightarrow J/\psi\Lambda$ proceeds on a proton embedded in a nuclear target.

⁶⁾And Λ hyperons, for which the kinematically allowed momentum interval looks like $1.286 \leq p_\Lambda \leq 4.522$ GeV/c, for instance, for $p_{K^-} = 10$ GeV/c [70].

For our purposes, we need the J/ψ energy spectrum $d\sigma_{K^-p \rightarrow J/\psi\Lambda}[\sqrt{s}, p_{J/\psi}]/dE_{J/\psi}$, arising from this reaction, taking place on a free target proton at rest, as a function of the J/ψ total energy $E_{J/\psi}$ belonging to the interval (13). It was calculated [70] to be:

$$\frac{d\sigma_{K^-p \rightarrow J/\psi\Lambda}[\sqrt{s}, p_{J/\psi}]}{dE_{J/\psi}} = \left(\frac{2\pi\sqrt{s}}{p_{K^-}p_{J/\psi}^*} \right) \frac{d\sigma_{K^-p \rightarrow J/\psi\Lambda}[\sqrt{s}, \theta_{J/\psi}^*(x_0)]}{d\Omega_{J/\psi}^*} \text{ for } E_{J/\psi}^{(2)}(0^\circ) \leq E_{J/\psi} \leq E_{J/\psi}^{(1)}(0^\circ). \quad (23)$$

Here, $d\sigma_{K^-p \rightarrow J/\psi\Lambda}(\sqrt{s}, \theta_{J/\psi}^*)/d\Omega_{J/\psi}^*$ is the on-shell differential cross section for the production of J/ψ meson in reaction (5) under the polar angle $\theta_{J/\psi}^*$ in the K^-p c.m.s. This cross section is assumed to have the standard exponential t -shape form, multiplied by the free total cross section $\sigma_{K^-p \rightarrow J/\psi\Lambda}(\sqrt{s})$ of the reaction $K^-p \rightarrow J/\psi\Lambda$. The latter one assumes the form [70]:

$$\sigma_{K^-p \rightarrow J/\psi\Lambda}(\sqrt{s}) = 7 \cdot 10^{-6} \cdot \sigma_{K^-p \rightarrow \phi\Lambda}(\sqrt{\tilde{s}}), \quad (24)$$

where the quantity $\sigma_{K^-p \rightarrow \phi\Lambda}(\sqrt{\tilde{s}})$ represents the free total cross section of the process $K^-p \rightarrow \phi\Lambda$ and the center-of-mass collision energies \sqrt{s} and $\sqrt{\tilde{s}}$ are linked by the relation:

$$\sqrt{\tilde{s}} = \sqrt{s} - m_{J/\psi} + m_\phi. \quad (25)$$

Here, the quantity m_ϕ is the vacuum ϕ meson mass. For the cross section $\sigma_{K^-p \rightarrow \phi\Lambda}(\sqrt{\tilde{s}})$ we have adopted the following parametrization:

$$\sigma_{K^-p \rightarrow \phi\Lambda}(\sqrt{\tilde{s}}) = B p_\phi^* e^{-\beta p_\phi^*}, \quad (26)$$

suggested in Ref. [74]. Here, the ϕ c.m. momentum p_ϕ^* is defined by the expression:

$$p_\phi^* = \frac{1}{2\sqrt{\tilde{s}}} \lambda(\tilde{s}, m_\phi^2, m_\Lambda^2) \quad (27)$$

and parameters B and β are: $B = 315.31 \mu\text{b}/(\text{GeV}/c)$, $\beta = 1.45 (\text{GeV}/c)^{-1}$. The expressions (23)–(27) will be used by us for calculating the free space J/ψ energy spectrum for incident resonant antikaon beam momenta of 9.417, 9.965 and 10.026 GeV/ c (see below) and the J/ψ excitation function near threshold.

As was noticed above (see Eq. (11)), the J/ψ mesons are produced at small angles with respect to the K^- beam direction at the considered initial K^- meson momenta. Therefore, in what follows, for calculation of the momentum differential cross section for J/ψ meson production in K^-A interactions from the direct process (5) we will use Eq. (33) from Ref. [70], which now reads:

$$\frac{d\sigma_{K^-A \rightarrow J/\psi X}^{(\text{dir})}(p_{K^-}, p_{J/\psi})}{dp_{J/\psi}} = 2\pi \left(\frac{Z}{A} \right) I_V[A, \sigma_{J/\psi N}] \int_{\cos 20^\circ}^1 d \cos \theta_{J/\psi} \left\langle \frac{d\sigma_{K^-p \rightarrow J/\psi\Lambda}(p_{K^-}, p_{J/\psi}, \theta_{J/\psi})}{dp_{J/\psi} d\Omega_{J/\psi}} \right\rangle_A, \quad (28)$$

where

$$I_V[A, \sigma] = 2\pi A \int_0^R r_\perp dr_\perp \int_{-\sqrt{R^2-r_\perp^2}}^{\sqrt{R^2-r_\perp^2}} dz \rho(\sqrt{r_\perp^2 + z^2}) \quad (29)$$

$$\times \exp \left[-A\sigma_{K^-N} \int_{-\sqrt{R^2-r_\perp^2}}^z \rho(\sqrt{r_\perp^2 + x^2}) dx - A\sigma \int_z^{\sqrt{R^2-r_\perp^2}} \rho(\sqrt{r_\perp^2 + x^2}) dx \right].$$

Here in Eq. (28), $\left\langle \frac{d\sigma_{K^-p \rightarrow J/\psi\Lambda}(p_{K^-}, p_{J/\psi}, \theta_{J/\psi})}{dp_{J/\psi} d\Omega_{J/\psi}} \right\rangle_A$ is the off-shell inclusive differential cross section for the production of J/ψ mesons with momentum $\mathbf{p}_{J/\psi}$ in reaction (5), averaged over the Fermi motion and binding energy of the protons in the nucleus (cf. Eq. (5) from Ref. [70]). The quantities $\rho(r)$ as well as $\sigma_{K^-N}^{\text{tot}}$ and $\sigma = \sigma_{J/\psi N}$, entering into Eq. (29), denote, respectively, the target nucleon density, normalized to unity, as well as the total cross section of the free K^-N interaction and $J/\psi N$ absorption cross section ⁷⁾. In our calculations we assume that the neutron and proton densities have the same radial shape $\rho(r)$. For it we have assumed an harmonic oscillator and a two-parameter Fermi distributions for ^{12}C and ^{184}W target nuclei, respectively. For the rest of notation see Ref. [70].

2.2. Two-step resonant J/ψ production processes

At K^- meson beam momenta below 10.2 GeV/c of interest, incident antikaons can produce the neutral $P_{cs}(4338)^0$, $P_{cs}(4455)^0$ and $P_{cs}(4468)^0$ pentaquark resonances with single strangeness $S = -1$ directly in the first inelastic collisions with intranuclear protons:

$$\begin{aligned} K^- + p &\rightarrow P_{cs}(4338)^0, \\ K^- + p &\rightarrow P_{cs}(4455)^0, \\ K^- + p &\rightarrow P_{cs}(4468)^0. \end{aligned} \quad (30)$$

Then the produced pentaquark resonances can decay into the final state $J/\psi\Lambda$, which will additionally contribute to the J/ψ yield in the $(K^-, J/\psi)$ reactions on protons and nuclei:

$$\begin{aligned} P_{cs}(4338)^0 &\rightarrow J/\psi + \Lambda, \\ P_{cs}(4455)^0 &\rightarrow J/\psi + \Lambda, \\ P_{cs}(4468)^0 &\rightarrow J/\psi + \Lambda. \end{aligned} \quad (31)$$

As above in the case of direct J/ψ meson production, at first, we consider here the charmonium production in the production/decay sequences (30)/(31), taking place on a free target proton at rest. According to [70], the free space total cross sections $\sigma_{K^-p \rightarrow P_{csi}^0 \rightarrow J/\psi\Lambda}(\sqrt{s}, \Gamma_{csi})$ for resonant charmonium production in these sequences can be represented as follows ⁸⁾:

$$\sigma_{K^-p \rightarrow P_{csi}^0 \rightarrow J/\psi\Lambda}(\sqrt{s}, \Gamma_{csi}) = \sigma_{K^-p \rightarrow P_{csi}^0}(\sqrt{s}, \Gamma_{csi}) \theta[\sqrt{s} - (m_{J/\psi} + m_\Lambda)] Br[P_{csi}^0 \rightarrow J/\psi\Lambda]. \quad (32)$$

Here, $\theta(x)$ is the step function and the quantities $Br[P_{csi}^0 \rightarrow J/\psi\Lambda]$ ($i = 1, 2, 3$) represent the branching ratios of the decays (31). In Eq. (32), the quantities $\sigma_{K^-p \rightarrow P_{csi}^0}(\sqrt{s}, \Gamma_{csi})$ are the total cross sections for production of the P_{csi}^0 resonances with the possible spin-parity quantum numbers $J^P = (1/2)^-$ for P_{cs1}^0 and P_{cs2}^0 , and $J^P = (3/2)^-$ for P_{cs3}^0 in reactions (30) ⁹⁾. These cross sections can be described, using the spectral functions $S_{csi}^0(\sqrt{s}, \Gamma_{csi})$ of resonances and knowing the branching fractions $Br[P_{csi}^0 \rightarrow K^-p]$ of their decays to the K^-p mode, as follows [70]:

$$\sigma_{K^-p \rightarrow P_{csi}^0}(\sqrt{s}, \Gamma_{csi}) = f_{csi} \left(\frac{\pi}{p_{K^-}^*} \right)^2 Br[P_{csi}^0 \rightarrow K^-p] S_{csi}^0(\sqrt{s}, \Gamma_{csi}) \Gamma_{csi}, \quad i = 1, 2, 3, \quad (33)$$

⁷⁾For which we use the values $\sigma_{K^-N}^{\text{tot}} = 22$ mb and $\sigma_{J/\psi N} = 3.5$ mb [70].

⁸⁾Here, $i = 1, 2, 3$ and P_{cs1}^0 , P_{cs2}^0 and P_{cs3}^0 stand for $P_{cs}(4338)^0$, $P_{cs}(4455)^0$ and $P_{cs}(4468)^0$ states, respectively. Analogously, Γ_{cs1} , Γ_{cs2} and Γ_{cs3} will denote in this exploratory study, correspondingly, the central values of their total decay widths, i.e.: $\Gamma_{cs1} = 7.0$ MeV, $\Gamma_{cs2} = 7.5$ MeV and $\Gamma_{cs3} = 5.2$ MeV.

⁹⁾Which might be assigned to them within the hadronic molecular scenario for their internal structure (see Introduction section above).

where the c.m. 3-momentum in the incoming K^-p channel, $p_{K^-}^*$, is defined by the formula

$$p_{K^-}^* = \frac{1}{2\sqrt{s}}\lambda(s, m_{K^-}^2, m_p^2) \quad (34)$$

and the ratios of the spin factors $f_{cs1} = 2$, $f_{cs2} = 2$, $f_{cs3} = 4$. In line with Ref. [70], we suppose that the free spectral functions $S_{csi}^0(\sqrt{s}, \Gamma_{csi})$ of the intermediate P_{csi}^0 resonances, entering into Eq. (33), are described by the non-relativistic Breit-Wigner distributions ¹⁰⁾:

$$S_{csi}^0(\sqrt{s}, \Gamma_{csi}) = \frac{1}{2\pi} \frac{\Gamma_{csi}}{(\sqrt{s} - M_{csi})^2 + \Gamma_{csi}^2/4}. \quad (35)$$

Inspection of Eqs. (32), (33) tells us that to evaluate the J/ψ production cross sections from the production/decay sequences (30)/(31), taking place on a vacuum proton (and on a bound in a nuclear medium proton), one needs to know the branching ratios $Br[P_{csi}^0 \rightarrow K^-p]$ and $Br[P_{csi}^0 \rightarrow J/\psi\Lambda]$ ($i=1, 2, 3$) of the P_{csi}^0 decays to the K^-p and $J/\psi\Lambda$ channels. We focus now on them.

The branching ratios $Br[P_{csi}^0 \rightarrow J/\psi\Lambda]$ of the decays (31) were not determined experimentally. Therefore, we must rely on the theoretical predictions for them as well as on the similarity of the behaviors and decay properties of the P_{cs} and P_c systems (cf. Introduction and Refs. [15, 35]). Thus, the decay rates of the modes $P_c^+ \rightarrow J/\psi p$ and $P_{cs}^0 \rightarrow J/\psi\Lambda^0$ are expressed in Ref. [15] in terms of the single model parameter Λ , which should be constrained from the future experiments, and these rates are comparable to each other. Model-dependent upper limits on branching fractions $Br[P_c(4312)^+ \rightarrow J/\psi p]$, $Br[P_c(4440)^+ \rightarrow J/\psi p]$ and $Br[P_c(4457)^+ \rightarrow J/\psi p]$ of several percent were set by the GlueX experiment [76] at JLab. Preliminary results from a factor of 10 more data, collected in the J/ψ -007 experiment [77] also at JLab, focused on the large t region ¹¹⁾ in searching for the LHCb hidden-charm pentaquarks [24], also observe no signals for them and set more stringent upper limits on the cross sections for production of the $P_c(4312)^+$, $P_c(4440)^+$ and $P_c(4457)^+$ states in γp collisions almost an order of magnitude below the respective GlueX limits [76]. With this, with upper limits on the branching fractions $Br[P_c(4312/4440/4457)^+ \rightarrow J/\psi p]$ already available from the GlueX experiment [76] and within the representation of these cross sections, in which they are proportional, respectively, to the $Br^2[P_c(4312/4440/4457)^+ \rightarrow J/\psi p]$, the upper limits on the above branching fractions, which are expected from the J/ψ -007 experiment [77], were estimated to be at the level of 1% in Ref. [78]. Based on the branching ratios and fractions measured by the LHCb and GlueX Collaborations, the authors of Ref. [79] obtain that a lower limit of $Br[P_c^+ \rightarrow J/\psi p]$ is of the order of 0.05% \sim 0.5%. Taking into account these findings as well as the fact that the ratios of the branching fractions $Br[P_c^+ \rightarrow J/\psi p]$ between three states $P_c(4312)^+$, $P_c(4440)^+$ and $P_c(4457)^+$ were predicted to be ~ 1 in Ref. [16], we adopted in our study [78] for the branching fractions of $P_c^+ \rightarrow J/\psi p$ decays for each individual P_c^+ state three following conservative options: $Br[P_c^+ \rightarrow J/\psi p] = 0.25, 0.5$ and 1%. With this and in view of the aforesaid, it is natural to assume for all branching ratios $Br[P_{csi}^0 \rightarrow J/\psi\Lambda]$ of the decays (31) the same three main options, namely: $Br[P_{csi}^0 \rightarrow J/\psi\Lambda] = 0.25, 0.5$ and 1% ($i=1, 2, 3$) as those given above and used for the $P_c^+ \rightarrow J/\psi p$ decays, and additional one with reduced value of 0.125% of these ratios in order to see better the size of their impact on the resonant J/ψ yield in $K^-p \rightarrow J/\psi\Lambda$, $K^{-12}\text{C} \rightarrow J/\psi X$ and $K^{-184}\text{W} \rightarrow J/\psi X$ reactions ¹²⁾. It is worth mentioning that the investigations in Refs. [34, 54] support in

¹⁰⁾In view of the fact that the $P_{cs}(4338)^0$ state is very close to the $\Xi_c^0\bar{D}^0$ and $\Xi_c^+D^-$ thresholds, its lineshape may be distorted from the conventional BW distribution due to the double threshold effects [29, 75]. But since the possible pole positions for the $P_{cs}(4338)^0$ (what concerns the masses and widths), found in [29, 75], are close (within the uncertainties) to those BW parameters determined in the LHCb analysis, the generation of the $P_{cs}(4338)^0$ shape with BW one carried out in the present work is reasonable enough for our exploratory purposes.

¹¹⁾In which the rather flat resonant production of J/ψ through the P_c^+ in photon-induced reactions on the protons is expected to be enhanced relative to the suppressed here mostly forward diffractive production.

¹²⁾It should be pointed out that in view of the aforementioned these options are more realistic than those of 3, 5, 10, 15 and 50% employed in Ref. [70] for the $P_{cs}(4459)^0 \rightarrow J/\psi\Lambda$ decays.

some sense such choice for the branching fractions of the decays (31). Thus, investigation of the strong decays of the $P_{cs}(4459)^0$ pentaquark, assuming that it is a pure S -wave $\Xi_c \bar{D}^*$ molecular state with two possible spin-parity assignments $J^P = (1/2)^-$ and $J^P = (3/2)^-$, has been performed in Ref. [34] through hadronic loops with the help of the effective Lagrangians. In comparison with the LHCb data [24], the S -wave $\Xi_c \bar{D}^*$ molecule with $J^P = (1/2)^-$ assignment for the $P_{cs}(4459)^0$ is supported by the study [34]. Using the results for the total decay width and for the partial width of the decay of the $P_{cs}(4459)^0$ with $J^P = (1/2)^-$ into the $J/\psi\Lambda$, the branching ratio of this decay could be evaluated at the level of 1%. Further, the author in Ref. [54], interpreting the pentaquark $P_{cs}(4459)^0$ observed by the LHCb Collaboration [24] as the hadronic molecule with the dominant S -wave channels $\Xi_c \bar{D}^*$ and $\Xi_c^* \bar{D}$ with the spin-parity combination $J^P = (3/2)^-$, predicted adopting the one-boson-exchange model that the partial decay width for the process $P_{cs}(4459)^0 \rightarrow J/\psi\Lambda$ is around 0.1 MeV in the resonance region. With this value and with the $P_{cs}(4459)^0$ resonance total decay width of about 20 MeV also predicted in [54] in this region, we obtain that the branching fraction $Br[P_{cs}(4459)^0 \rightarrow J/\psi\Lambda]$ amounts to 0.5%. Moreover, 1% branching ratio of the $P_{cs}(4459)^0 \rightarrow J/\psi\Lambda$ decay was chosen as the main one in Ref. [69]. In previous works [69, 70], devoted to the study of the $P_{cs}(4459)^0$ resonance production in antikaon-induced reactions on protons and nuclei, the value of 0.01% was used for the branching fraction $Br[P_{cs}(4459)^0 \rightarrow K^-p]$. It was chosen to be similar to that characterizing [80] the $P_c^0 \rightarrow \pi^-p$ decay. Based on the molecular scenario, the partial decay widths of the $P_{cs}(4459)^0$ with $J^P = (1/2)^-$ and $J^P = (3/2)^-$ into K^-p final state via hadronic loops were evaluated in Ref. [71] to be of the order of 2.05 and 0.24 KeV, respectively. If we adopt an experimental magnitude of 17.3 MeV for the $P_{cs}(4459)^0$ total decay width, we obtain with the above partial decay widths that the branching fraction $Br[P_{cs}(4459)^0 \rightarrow K^-p]$ would be $\sim 0.01\%$ and 0.001% for the $P_{cs}(4459)^0$ with $J^P = (1/2)^-$ and $J^P = (3/2)^-$, correspondingly. In line with the aforementioned, it is also natural to employ in our cross-section calculations for the branching ratios $Br[P_{csi}^0 \rightarrow K^-p]$ ($i=1, 2, 3$) the main value of 0.01%. To see the effect of the branching ratios on the resonant J/ψ yield in the reactions of interest, we will also use for them in these calculations the value of 0.001%.

Before going further, we determine the resonant J/ψ energy distributions $d\sigma_{K^-p \rightarrow P_{csi}^0 \rightarrow J/\psi\Lambda}[\sqrt{s}, p_{J/\psi}]/dE_{J/\psi}$ ($i=1, 2, 3$) from the two-step processes (30)/(31), proceeding on the free target proton at rest, in addition to that (23) from the background $K^-p \rightarrow J/\psi\Lambda$ reaction. The energy-momentum conservation in these processes leads to the conclusion that the kinematical characteristics of J/ψ mesons produced in them and in this reaction are the same at given incident K^- meson momentum. The results of the calculations, performed in Ref. [70] assuming that the decays of the P_{csi}^0 to the $J/\psi\Lambda$ are dominated by the lowest partial waves with relative orbital angular momentum $L=0$, show that these distributions can be represented in the following way:

$$\frac{d\sigma_{K^-p \rightarrow P_{csi}^0 \rightarrow J/\psi\Lambda}[\sqrt{s}, p_{J/\psi}]}{dE_{J/\psi}} = \sigma_{K^-p \rightarrow P_{csi}^0}(\sqrt{s}, \Gamma_{csi})\theta[\sqrt{s} - (m_{J/\psi} + m_\Lambda)] \times \quad (36)$$

$$\times \left(\frac{\sqrt{s}}{2p_{K^-} p_{J/\psi}^*} \right) Br[P_{csi}^0 \rightarrow J/\psi\Lambda] \text{ for } E_{J/\psi}^{(2)}(0^\circ) \leq E_{J/\psi} \leq E_{J/\psi}^{(1)}(0^\circ).$$

Eq. (36) shows that the free space J/ψ energy distributions, which arise from the production/decay chains (30)/(31), exhibit a totally flat behavior within the allowed energy range (13).

For calculation of the J/ψ inclusive differential cross section (momentum spectrum) arising from the production and decay of the intermediate resonances P_{csi}^0 in K^-A collisions we will use the following expression based on Eq. (78) from Ref. [70]:

$$\frac{d\sigma_{K^-A \rightarrow J/\psi X}^{(\text{sec},i)}(p_{K^-}, p_{J/\psi})}{dp_{J/\psi}} = 2\pi \left(\frac{Z}{A} \right) I_V[A, \sigma_{P_{csi}^0 N}^{\text{in}}] \quad (37)$$

$$\times \int_{\cos 20^\circ}^1 d \cos \theta_{J/\psi} \left\langle \frac{d\sigma_{K^-p \rightarrow P_{csi}^0 \rightarrow J/\psi\Lambda}(p_{K^-}, p_{J/\psi}, \theta_{J/\psi})}{dp_{J/\psi} d\Omega_{J/\psi}} \right\rangle_A, \quad i = 1, 2, 3;$$

where $\left\langle \frac{d\sigma_{K^-p \rightarrow P_{csi}^0 \rightarrow J/\psi\Lambda}(p_{K^-}, p_{J/\psi}, \theta_{J/\psi})}{dp_{J/\psi} d\Omega_{J/\psi}} \right\rangle_A$ is the off-shell inclusive differential cross section for the production of J/ψ mesons with momentum $\mathbf{p}_{J/\psi}$ in production/decay chain $K^-p \rightarrow P_{csi}^0 \rightarrow J/\psi\Lambda$, averaged over the Fermi motion and binding energy of the protons in the nucleus (cf. Eq. (71) from Ref. [70]). The quantity $I_V[A, \sigma_{P_{csi}^0 N}^{\text{in}}]$ in Eq. (37) is defined above by Eq. (29), in which one needs to make the substitution $\sigma \rightarrow \sigma_{P_{csi}^0 N}^{\text{in}}$. Here, $\sigma_{P_{csi}^0 N}^{\text{in}}$ is the P_{csi}^0 -nucleon inelastic total cross section. For this cross section we will use in our calculations the same value of 23.7 mb as that adopted in Ref. [70] for the inelastic cross section $\sigma_{P_{cs}(4459)^0 N}^{\text{in}}$ and obtained here in the molecular picture of the $P_{cs}(4459)^0$.

3. Results and discussion

The direct non-resonant J/ψ production total cross section (24) on the target proton at rest (black solid curves), the total cross section for the resonant J/ψ production in the processes (30)/(31) calculated on the basis of Eq. (32) for the considered spin-parity assignments of the P_{csi}^0 resonances ($i = 1, 2, 3$) as well as for the branching ratios $Br[P_{csi}^0 \rightarrow K^-p] = 0.01\%$ and $Br[P_{csi}^0 \rightarrow J/\psi\Lambda] = 0.125, 0.25, 0.5$ and 1% for all three P_{csi}^0 states (red short-dashed curves) and the combined (non-resonant plus resonant) J/ψ production total cross section (blue dotted curves) are presented in Fig. 1 as functions of the K^- meson laboratory momentum. The same as that shown in Fig. 1, but determined for the three branching ratios $Br[P_{csi}^0 \rightarrow K^-p] = 0.001\%$, is presented in Fig. 2 to see the sensitivity of the combined J/ψ production total cross section to these ratios. One can see from these figures that the $P_{cs}(4338)^0$ state as well as $P_{cs}(4455)^0$ and $P_{cs}(4468)^0$ resonances manifest itself, respectively, as distinct narrow single peak as well as two narrow overlapping peaks at antikaon resonant momenta $p_{K^-}^{\text{R1}} = 9.417$ GeV/c as well as at $p_{K^-}^{\text{R2}} = 9.965$ GeV/c and $p_{K^-}^{\text{R3}} = 10.026$ GeV/c in the combined cross section, only if $Br[P_{csi}^0 \rightarrow K^-p] = 0.01\%$ and $Br[P_{csi}^0 \rightarrow J/\psi\Lambda] = 1\%$ for all three P_{csi}^0 states. In this case, in the resonance regions the resonant contributions are much larger than the non-resonant ones of about 0.5 nb and the peak values of the strengths of these three peaks reach a well measurable values $\sim 2-3$ nb. Hence, the background reaction $K^-p \rightarrow J/\psi\Lambda$ will not influence the direct observation of the hidden-charm strange pentaquarks $P_{cs}(4338)^0$, $P_{cs}(4455)^0$ and $P_{cs}(4468)^0$ production at these momenta and in this case. If $Br[P_{csi}^0 \rightarrow J/\psi\Lambda] \leq 0.5\%$, then the resonant J/ψ yields are comparable to (or are less than) the non-resonant ones in the resonance regions. As a result, the $P_{cs}(4338)^0$, $P_{cs}(4455)^0$ and $P_{cs}(4468)^0$ states do not appear as pronounced peaks in the combined cross section. This implies that will be hard to measure in this case the P_{csi}^0 pentaquark states in J/ψ total production cross section on a proton target in the antikaon-induced reactions. From Fig. 2 we see that the resonant J/ψ production cross section is small compared to the non-resonant contribution at all antikaon momenta considered for four adopted values for the three branching ratios $Br[P_{csi}^0 \rightarrow J/\psi\Lambda]$, when $Br[P_{csi}^0 \rightarrow K^-p] = 0.001\%$. In this case, the combined total cross section of the reaction $K^-p \rightarrow J/\psi\Lambda$ has no distinct peak structures, corresponding to the P_{csi}^0 states, and it is practically not distinguished from that for the background reaction. In view of the above, it is natural to expect that the P_{csi}^0 signals could be well distinguished from the background reaction via the detailed scan of the J/ψ total production cross section on a proton target in the near-threshold K^- momentum regions around resonant momenta of 9.417, 9.965 and 10.026 GeV/c in the future dedicated experiment at J-PARC facility, if branching ratios $Br[P_{csi}^0 \rightarrow K^-p] \sim 0.01\%$ and $Br[P_{csi}^0 \rightarrow J/\psi\Lambda] \sim 1\%$. To see experimentally such signals in the combined total cross section of the reaction $K^-p \rightarrow J/\psi\Lambda$, it is enough to have the K^- momentum resolution (and the momentum binning) of the order of 5 MeV/c. Thus, the c.m.

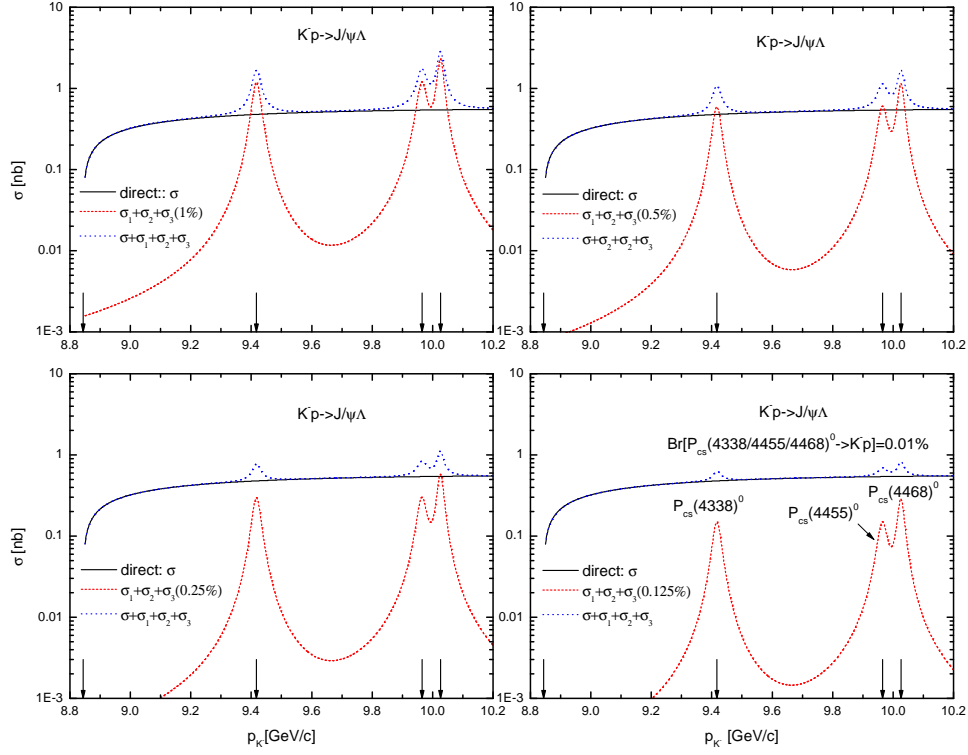


Figure 1: (Color online.) The non-resonant total cross section σ for the reaction $K^-p \rightarrow J/\psi\Lambda$ (black solid curve), calculated on the basis of Eqs. (24)–(27). Incoherent sum (blue dotted curve) of it and the sum $\sigma_1 + \sigma_2 + \sigma_3$ (red short-dashed curve) of the total cross sections σ_1 , σ_2 and σ_3 for the resonant J/ψ production in the processes $K^-p \rightarrow P_{cs}(4338)^0 \rightarrow J/\psi\Lambda$, $K^-p \rightarrow P_{cs}(4455)^0 \rightarrow J/\psi\Lambda$ and $K^-p \rightarrow P_{cs}(4468)^0 \rightarrow J/\psi\Lambda$, calculated in line with Eq. (32) assuming that the resonances $P_{cs}(4338)^0$, $P_{cs}(4455)^0$ and $P_{cs}(4468)^0$ with the spin-parity quantum numbers $J^P = (1/2)^-$, $J^P = (1/2)^-$ and $J^P = (3/2)^-$ decay to the K^-p and $J/\psi\Lambda$ channels with all three individual branching fractions 0.01% and 1, 0.5, 0.25 and 0.125% (respectively, upper left, upper right, lower left and lower right panels), as functions of the incident K^- meson momentum. The left and three right arrows indicate, correspondingly, the threshold momentum $p_{K^-}^{\text{th}} = 8.844$ GeV/c for the reaction $K^-p \rightarrow J/\psi\Lambda$, taking place on a free target proton being at rest, and the resonant antikaon momenta $p_{K^-}^{\text{R1}} = 9.417$ GeV/c, $p_{K^-}^{\text{R2}} = 9.965$ GeV/c and $p_{K^-}^{\text{R3}} = 10.026$ GeV/c.

energy ranges $M_{c_{si}} - \Gamma_{c_{si}}/2 < \sqrt{s} < M_{c_{si}} + \Gamma_{c_{si}}/2$ ($i=1, 2, 3$) correspond to the laboratory antikaon momentum regions of 9.401 GeV/c $< p_{K^-} < 9.433$ GeV/c, 9.947 GeV/c $< p_{K^-} < 9.982$ GeV/c and 10.013 GeV/c $< p_{K^-} < 10.038$ GeV/c, i.e. $\Delta p_{K^-} = 32, 35$ and 25 MeV/c for the $P_{cs}(4338)^0$, $P_{cs}(4455)^0$ and $P_{cs}(4468)^0$, respectively. This means that to resolve the peaks in the upper left panel of Fig. 1 the K^- beam momentum resolution (and the momentum bin size) of the order of 5 MeV/c are required. One may hope that this requirement will be satisfied at the K10 beam line at the J-PARC facility [72]. To further motivate the conducting of the relevant experiment at this facility, it is important to estimate the expected yields of the P_{csi}^0 signals from the reactions $K^-p \rightarrow P_{csi}^0 \rightarrow J/\psi\Lambda$, $J/\psi \rightarrow e^+e^-$, $\Lambda \rightarrow p\pi^-$ at least in the case, corresponding to the upper left panel of Fig. 1. Assuming incident antikaon beam intensity $\sim 10^6$ K^-/s in the peak antikaon momenta and 4g/cm^2 (57 cm) for the thickness of the liquid hydrogen target [72], one could reach

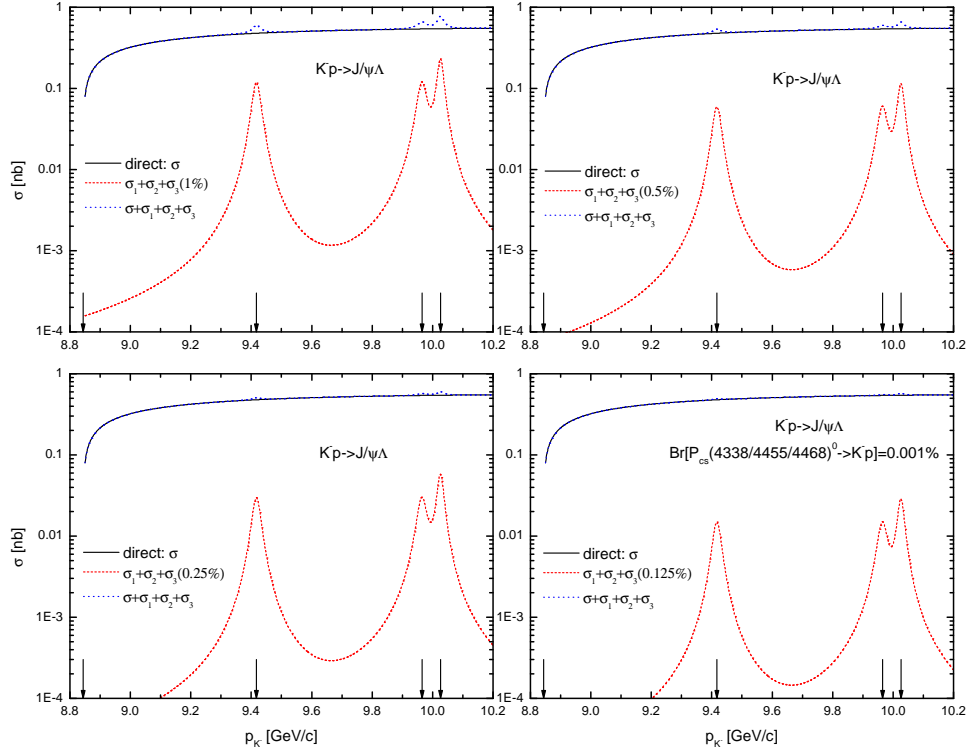


Figure 2: (Color online.) The same as in Fig. 1, but calculated for all three branching ratios of P_{csi}^0 ($i = 1, 2, 3$) decays to the K^-p mode of 0.001%.

an integrated luminosity of 76 pb^{-1} for a year of data taking. For the pentaquark yield (for the total number of the P_{csi}^0 events) estimates in a one-year beam time, one needs to multiply the above luminosity by the P_{csi}^0 production cross sections of 1.2, 1.2 and 2.3 nb at resonant K^- momenta of 9.417, 9.965 and 10.026 GeV/c as well as by the detection efficiency and by the appropriate branching ratios $Br[J/\psi \rightarrow e^+e^-] \approx 6\%$ and $Br[\Lambda \rightarrow p\pi^-] \approx 64\%$. Even with a relatively low (and realistic) 10% detection efficiency, we estimate about of 350, 350 and 670 events per year for the $P_{cs}(4338)^0$, $P_{cs}(4455)^0$ and $P_{cs}(4468)^0$ signals, respectively. For elastic (background) $J/\psi\Lambda$ production in the reaction $K^-p \rightarrow J/\psi\Lambda$ we have $\sigma = 0.54 \text{ nb}$ at considered K^- momenta. This leads to ≈ 160 events per year. We see that the elastic background is sufficiently small compared to the resonant yields. Therefore, highly intense, energetic and resolution K^- beam, which will be available at this beam line, should allow to get a definite result for or against the existence of the genuine $P_{cs}(4338)^0$ pentaquark state in the nature and the presence of two resonances in the peak of the $J/\psi\Lambda$ event distribution, associated to the $P_{cs}(4459)^0$, through the scan of the J/ψ total production cross section on a proton target in the resonance regions, only if branching ratios $Br[P_{csi}^0 \rightarrow K^-p] \sim 0.01\%$ and $Br[P_{csi}^0 \rightarrow J/\psi\Lambda] \sim 1\%$. It is obvious that to see the P_{csi}^0 pentaquarks experimentally in the cases, when more "softer" constraints than those given above are imposed on the branching ratios $Br[P_{csi}^0 \rightarrow K^-p]$ and $Br[P_{csi}^0 \rightarrow J/\psi\Lambda]$, one needs to consider such observable, which is appreciably sensitive to the P_{cs}^0 signal in some region of the available phase space. For instance, the large t region of the differential cross section $d\sigma/dt$ in the J/ψ -007 experiment [77], where the t -dependence of the background J/ψ meson production is suppressed while its resonant production is rather flat. This is also supported by the findings of Refs. [81–83].

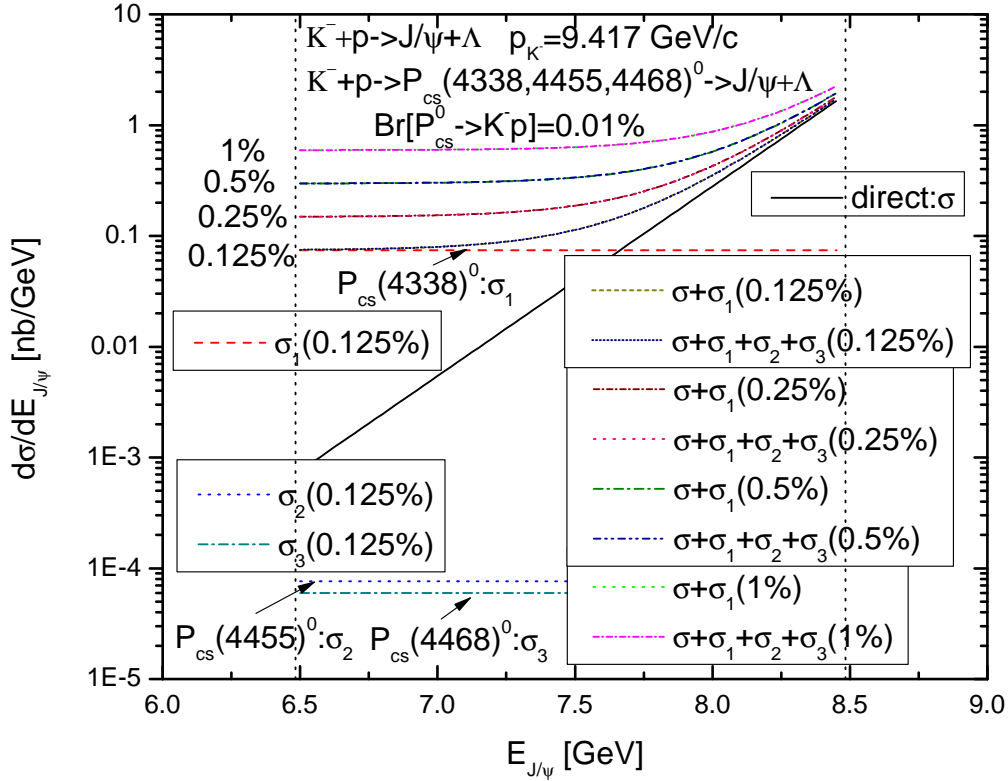


Figure 3: (Color online.) The direct non-resonant J/ψ energy distribution in the free space elementary process $K^-p \rightarrow J/\psi\Lambda$, calculated in line with Eq. (23) at initial K^- meson resonant momentum of 9.417 GeV/c in the laboratory system (black solid curve). The resonant J/ψ energy distributions in the two-step processes $K^-p \rightarrow P_{cs}(4338)^0 \rightarrow J/\psi\Lambda$, $K^-p \rightarrow P_{cs}(4455)^0 \rightarrow J/\psi\Lambda$ and $K^-p \rightarrow P_{cs}(4468)^0 \rightarrow J/\psi\Lambda$, calculated in line with Eq. (36) at the same incident antikaon momentum of 9.417 GeV/c assuming that the resonances $P_{cs}(4338)^0$, $P_{cs}(4455)^0$, $P_{cs}(4468)^0$ with the spin-parity assignments $J^P = (1/2)^-$, $J^P = (1/2)^-$, $J^P = (3/2)^-$, correspondingly, all decay to the K^-p and $J/\psi\Lambda$ modes with branching fractions of 0.01% and 0.125% (respectively, red dashed, blue dotted, dark cyan dashed-dotted curves). Incoherent sum of the direct non-resonant J/ψ energy distribution and resonant ones, calculated supposing that the resonances $P_{cs}(4338)^0$ as well as $P_{cs}(4338)^0$, $P_{cs}(4455)^0$, $P_{cs}(4468)^0$ with the same spin-parity combinations all decay to the K^-p and $J/\psi\Lambda$ with branching fractions 0.01% and 0.125, 0.25, 0.5, 1% (respectively, dark yellow short-dashed, wine short-dashed-dotted, olive dashed-dotted, green dotted as well as navy short-dotted, pink dotted, royal dashed-dotted-dotted, magenta short-dashed-dotted curves), all as functions of the total J/ψ energy $E_{J/\psi}$ in the laboratory system. The vertical dotted lines indicate the range of J/ψ allowed energies in this system ($6.483 \leq E_{J/\psi} \leq 8.484$ GeV) for the considered direct non-resonant and resonant J/ψ production off a free target proton at rest at given initial K^- meson resonant momentum of 9.417 GeV/c.

Accounting for the above-mentioned, we focus now on the J/ψ energy distribution from the considered $K^-p \rightarrow J/\psi\Lambda$ elementary reaction. Our model allows one to calculate the direct non-resonant J/ψ energy distribution from this reaction, the resonant ones from the production/decay sequences (30)/(31), proceeding on the free target proton being at rest. They were calculated in line with Eqs. (23), (36), respectively, for incident antikaon resonant momenta of 9.417, 9.965

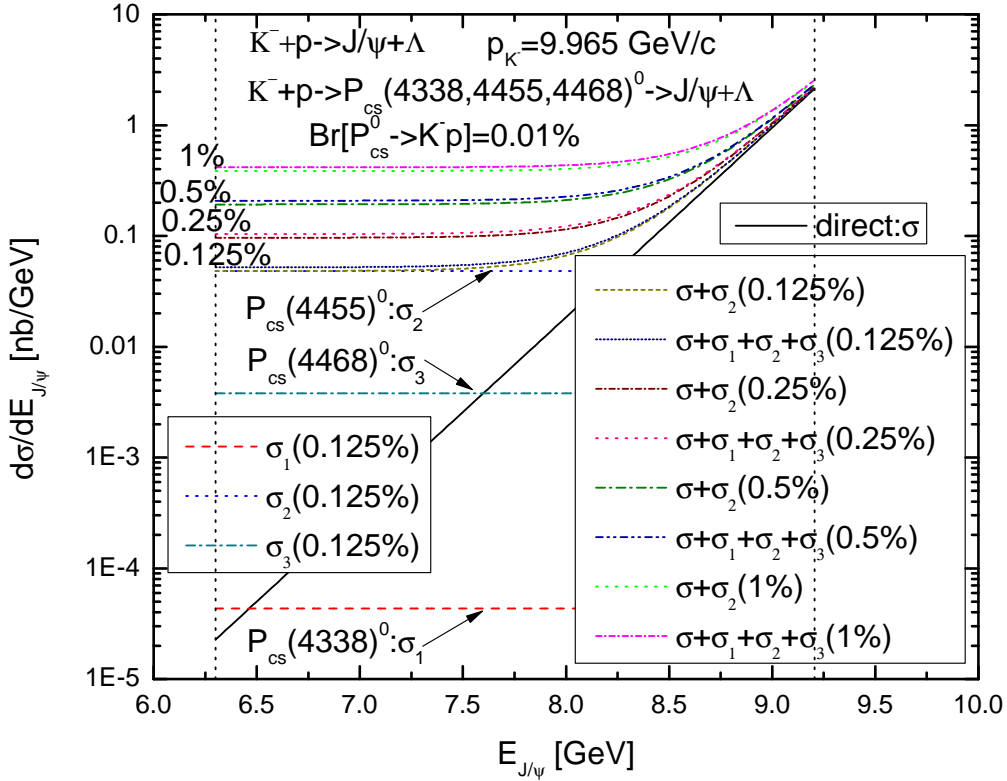


Figure 4: (Color online.) The direct non-resonant J/ψ energy distribution in the free space elementary process $K^-p \rightarrow J/\psi\Lambda$, calculated in line with Eq. (23) at initial K^- meson resonant momentum of 9.965 GeV/c in the laboratory system (black solid curve). The resonant J/ψ energy distributions in the two-step processes $K^-p \rightarrow P_{cs}(4338)^0 \rightarrow J/\psi\Lambda$, $K^-p \rightarrow P_{cs}(4455)^0 \rightarrow J/\psi\Lambda$ and $K^-p \rightarrow P_{cs}(4468)^0 \rightarrow J/\psi\Lambda$, calculated in line with Eq. (36) at the same incident antikaon momentum of 9.965 GeV/c assuming that the resonances $P_{cs}(4338)^0$, $P_{cs}(4455)^0$, $P_{cs}(4468)^0$ with the spin-parity assignments $J^P = (1/2)^-$, $J^P = (1/2)^-$, $J^P = (3/2)^-$, correspondingly, all decay to the K^-p and $J/\psi\Lambda$ modes with branching fractions of 0.01% and 0.125% (respectively, red dashed, blue dotted, dark cyan dashed-dotted curves). Incoherent sum of the direct non-resonant J/ψ energy distribution and resonant ones, calculated supposing that the resonances $P_{cs}(4455)^0$ as well as $P_{cs}(4338)^0$, $P_{cs}(4455)^0$, $P_{cs}(4468)^0$ with the same spin-parity combinations all decay to the K^-p and $J/\psi\Lambda$ with branching fractions 0.01% and 0.125, 0.25, 0.5, 1% (respectively, dark yellow short-dashed, wine short-dashed-dotted, olive dashed-dotted, green dotted as well as navy short-dotted, pink dotted, royal dashed-dotted-dotted, magenta short-dashed-dotted curves), all as functions of the total J/ψ energy $E_{J/\psi}$ in the laboratory system. The vertical dotted lines indicate the range of J/ψ allowed energies in this system ($6.300 \leq E_{J/\psi} \leq 9.205$ GeV) for the considered direct non-resonant and resonant J/ψ production off a free target proton at rest at given initial K^- meson resonant momentum of 9.965 GeV/c.

and 10.026 GeV/c. The resonant J/ψ energy distributions were determined for the employed spin-parity assignments of the $P_{cs}(4338)^0$, $P_{cs}(4455)^0$, $P_{cs}(4468)^0$ resonances for branching fractions $Br[P_{csi}^0 \rightarrow K^-p] = 0.01\%$ and $Br[P_{csi}^0 \rightarrow J/\psi\Lambda] = 0.125\%$ for all three states. These dependencies, together with the incoherent sum of the non-resonant J/ψ energy distribution and resonant ones, calculated supposing that all the resonances $P_{cs}(4338)^0$ and P_{csi}^0 ($i = 1, 2, 3$), $P_{cs}(4455)^0$ and P_{csi}^0

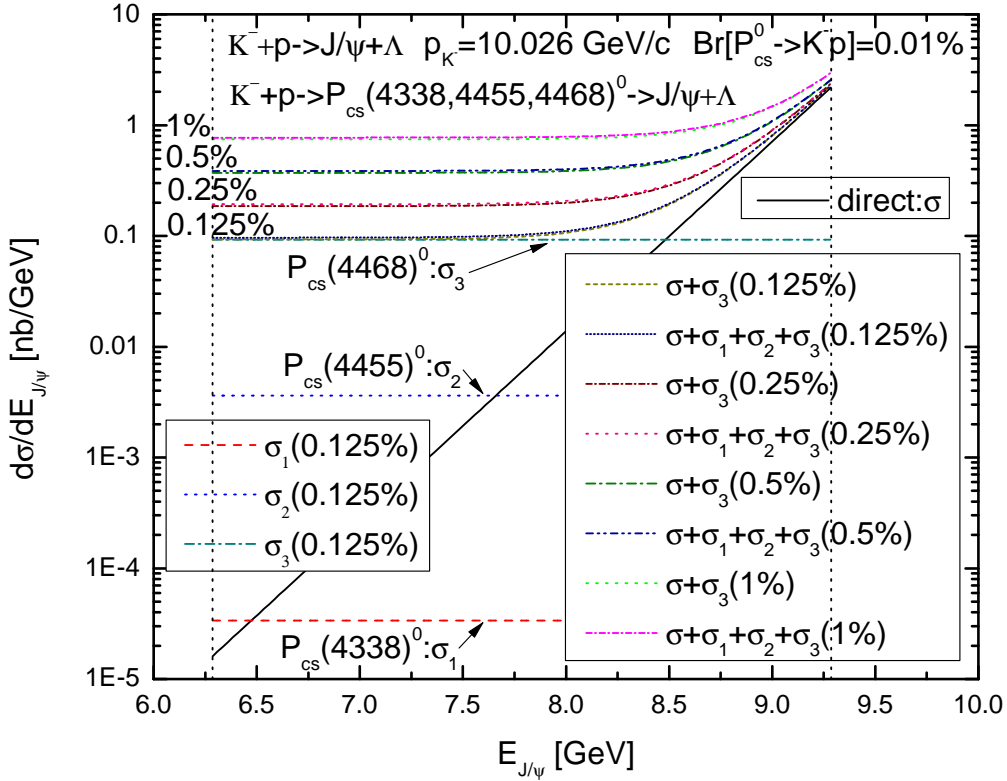


Figure 5: (Color online.) The direct non-resonant J/ψ energy distribution in the free space elementary process $K^-p \rightarrow J/\psi\Lambda$, calculated in line with Eq. (23) at initial K^- meson resonant momentum of 10.026 GeV/c in the laboratory system (black solid curve). The resonant J/ψ energy distributions in the two-step processes $K^-p \rightarrow P_{cs}(4338)^0 \rightarrow J/\psi\Lambda$, $K^-p \rightarrow P_{cs}(4455)^0 \rightarrow J/\psi\Lambda$ and $K^-p \rightarrow P_{cs}(4468)^0 \rightarrow J/\psi\Lambda$, calculated in line with Eq. (36) at the same incident antikaon momentum of 10.026 GeV/c assuming that the resonances $P_{cs}(4338)^0$, $P_{cs}(4455)^0$, $P_{cs}(4468)^0$ with the spin-parity assignments $J^P = (1/2)^-$, $J^P = (1/2)^-$, $J^P = (3/2)^-$, correspondingly, all decay to the K^-p and $J/\psi\Lambda$ modes with branching fractions of 0.01% and 0.125% (respectively, red dashed, blue dotted, dark cyan dashed-dotted curves). Incoherent sum of the direct non-resonant J/ψ energy distribution and resonant ones, calculated supposing that the resonances $P_{cs}(4468)^0$ as well as $P_{cs}(4338)^0$, $P_{cs}(4455)^0$, $P_{cs}(4468)^0$ with the same spin-parity combinations all decay to the K^-p and $J/\psi\Lambda$ with branching fractions 0.01% and 0.125, 0.25, 0.5, 1% (respectively, dark yellow short-dashed, wine short-dashed-dotted, olive dashed-dotted, green dotted as well as navy short-dotted, pink dotted, royal dashed-dotted-dotted, magenta short-dashed-dotted curves), all as functions of the total J/ψ energy $E_{J/\psi}$ in the laboratory system. The vertical dotted lines indicate the range of J/ψ allowed energies in this system ($6.286 \leq E_{J/\psi} \leq 9.280$ GeV) for the considered direct non-resonant and resonant J/ψ production off a free target proton at rest at given initial K^- meson resonant momentum of 10.026 GeV/c.

($i = 1, 2, 3$), $P_{cs}(4468)^0$ and P_{csi}^0 ($i = 1, 2, 3$) decay to the $J/\psi\Lambda$ final state with four adopted options for the branching ratios $Br[P_{csi}^0 \rightarrow J/\psi\Lambda]$, as functions of the J/ψ total energy $E_{J/\psi}$ are shown, respectively, in Figs. 3, 4, 5. The same as that shown in these figures, but calculated for the three branching ratios $Br[P_{csi}^0 \rightarrow K^-p] = 0.001\%$, is presented, respectively, in Figs. 6, 7, 8 to see the sensitivity of the combined J/ψ energy distribution to these ratios. It can be seen

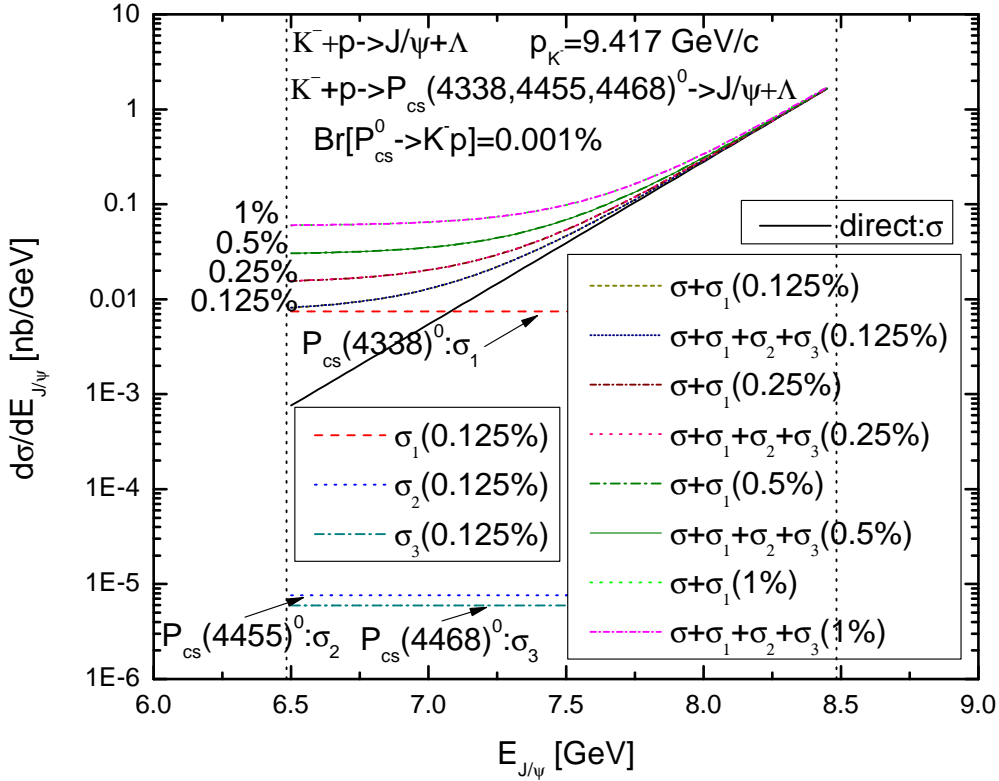


Figure 6: (Color online.) The same as in Fig. 3, but calculated for all three branching ratios of P_{csi}^0 ($i = 1, 2, 3$) decays to the K^-p mode of 0.001%.

from all these figures that while the resonant J/ψ production differential cross sections show a quite flat behavior at all allowed energies $E_{J/\psi}$, the non-resonant cross section drops quickly as the energy $E_{J/\psi}$ decreases. At incident K^- meson resonant momenta of 9.417, 9.965 and 10.026 GeV/c of our interest and in the case when $Br[P_{csi}^0 \rightarrow K^-p] = 0.01\%$ ($i = 1, 2, 3$), its strength is essentially larger than those of the resonant J/ψ production cross sections, calculated for the value of the branching ratios $Br[P_{csi}^0 \rightarrow J/\psi\Lambda] = 0.125\%$, for "high" allowed J/ψ total energies greater, correspondingly, than $\approx 7.75, 8.25$ and 8.5 GeV. Whereas at "low" J/ψ total energies (below, respectively, 7.75, 8.25 and 8.5 GeV) the contribution from the resonance, decaying to the $J/\psi\Lambda$ mode with the branching ratio of 0.125%, with the centroid, correspondingly, at momenta of 9.417, 9.965 and 10.026 GeV/c, is much larger than the non-resonant one. When $Br[P_{csi}^0 \rightarrow K^-p] = 0.001\%$, analogous J/ψ total energies are somewhat smaller, and they, respectively, are $\approx 7.25, 7.75$ and 8.0 GeV. Thus, for example, in the first and second cases (what concerns the branching ratios $Br[P_{csi}^0 \rightarrow K^-p]$ considered), for the J/ψ mesons with total energies about of 7.0 and 6.5 GeV their resonant production cross section, calculated for the branching fraction of 0.125% of its decay to the $J/\psi\Lambda$, is enhanced compared to the non-resonant one by sizeable factors about of one, two and three order of magnitude at incident antikaon momenta of 9.417, 9.965 and 10.026 GeV/c, respectively. Furthermore, this contribution is also essentially larger than those, arising from the decays of another two pentaquarks to the $J/\psi\Lambda$ with the branching ratios $Br[P_{csi}^0 \rightarrow J/\psi\Lambda] = 0.125\%$, at the aforementioned "low" J/ψ total energies. As a consequence, for each K^- beam momentum considered the J/ψ meson combined energy distribution, appearing from the direct J/ψ meson production and from the decay of the pentaquark resonance located at this momentum to the

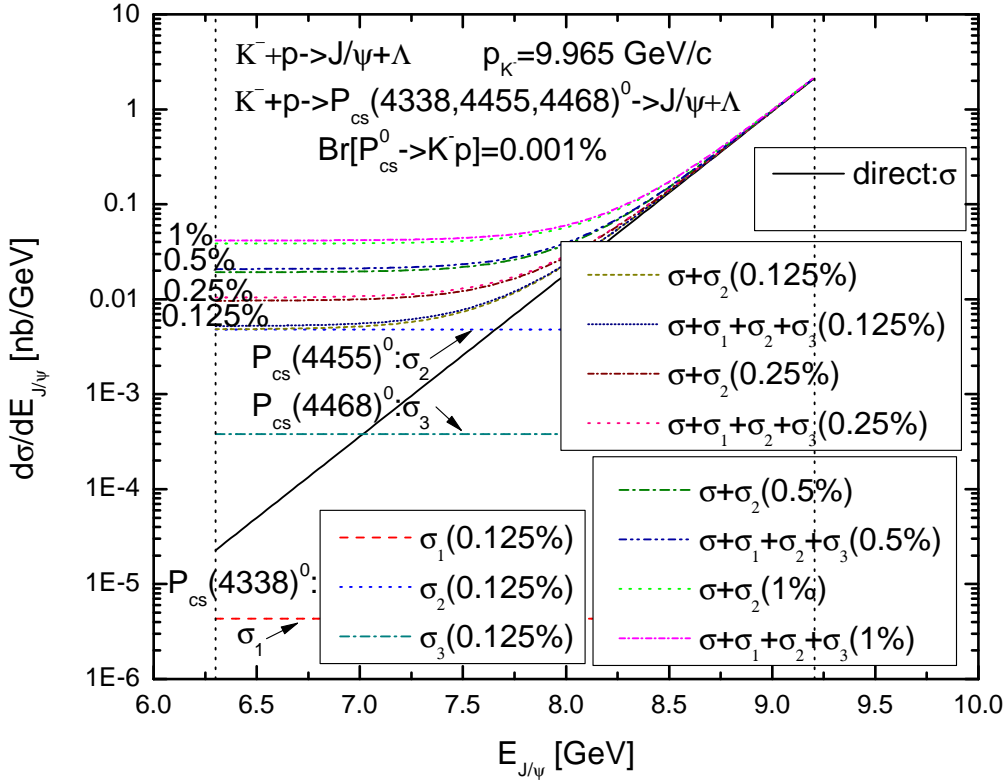


Figure 7: (Color online.) The same as in Fig. 4, but calculated for all three branching ratios of P_{csi}^0 ($i = 1, 2, 3$) decays to the K^-p mode of 0.001%.

$J/\psi\Lambda$ channel, reveals here a clear sensitivity to the employed variations in the branching ratio of this decay. Thus, for instance, for the J/ψ mesons with total energy of 6.5 GeV and for the lowest incident antikaon momentum of 9.417 GeV/c this J/ψ combined distribution is enhanced for the values of this ratio of 0.125, 0.25, 0.5, 1% by substantial factors of about 10.0, 20.0, 37.5, 80.0, respectively, as compared to that from the directly produced J/ψ mesons in the case when $Br[P_{csi}^0 \rightarrow K^-p] = 0.001\%$. And for the highest initial K^- meson momentum of 10.026 GeV/c of our interest, at which the resonance $P_{cs}(4468)^0$ appears as a weak peak structure in the total cross section of the exclusive reaction $K^-p \rightarrow J/\psi\Lambda$ only if $Br[P_{csi}^0 \rightarrow J/\psi\Lambda] = 1\%$, the analogous factors become much larger and they are of about $0.25 \cdot 10^3$, $0.5 \cdot 10^3$, $1 \cdot 10^3$, $2 \cdot 10^3$, respectively. Similarly, for the J/ψ mesons with total energy of 7.0 GeV, for incident K^- meson momenta of 9.417 and 10.026 GeV/c these factors are of about 13, 25, 50, 100 and $0.35 \cdot 10^3$, $0.7 \cdot 10^3$, $1.3 \cdot 10^3$, $2.6 \cdot 10^3$, correspondingly, if $Br[P_{csi}^0 \rightarrow K^-p] = 0.01\%$. Moreover, what is important, one can see that the above "partial" combined energy distribution of the J/ψ mesons, calculated at given values of the branching ratios $Br[P_{csi}^0 \rightarrow K^-p]$ and $Br[P_{csi}^0 \rightarrow J/\psi\Lambda]$, is practically indistinguishable from their "total" combined energy distribution, arising from the direct and resonant J/ψ meson production through all production/decay sequences (30)/(31), and determined at the same values of these branching ratios. This means that the differences between the combined results, obtained by using a value of the branching fractions of the decays $P_{csi}^0 \rightarrow J/\psi\Lambda$ of 0.125% and the non-resonant background, as well as between the combined results, determined by employing the values of the branching ratios of these decays of 0.125 and 0.25%, 0.25 and 0.5%, 0.5 and 1%, are quite large and experimentally measurable at "low" J/ψ total energies and for both adopted options for the

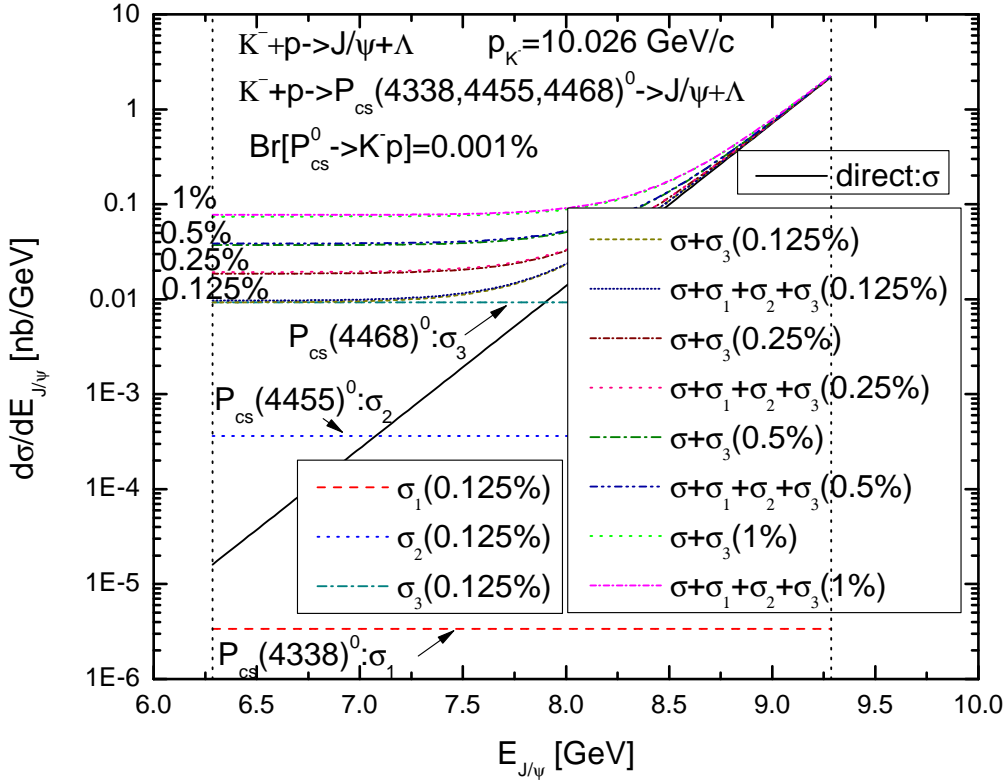


Figure 8: (Color online.) The same as in Fig. 5, but calculated for all three branching ratios of P_{csi}^0 ($i = 1, 2, 3$) decays to the K^-p mode of 0.001%.

branching fractions $Br[P_{csi}^0 \rightarrow K^-p]$ ($i = 1, 2, 3$). Furthermore, for each initial antikaon resonant momentum considered the observation here of the specific hidden-charm LHCb pentaquark with strangeness will be practically not influenced by the presence of the another two strange hidden-charm pentaquark states and by the background reaction. Since the J/ψ production differential cross sections have a small absolute values ~ 0.01 – 0.1 nb/GeV and ~ 0.1 – 1.0 nb/GeV at "low" J/ψ total energies $E_{J/\psi}$ for branching fractions $Br[P_{csi}^0 \rightarrow K^-p] = 0.001$ and 0.01%, respectively, their measurement requires both high luminosities and large-acceptance detectors. Such measurement might be performed in the near future at the J-PARC facility within the planned here experiments at the K10 beam line [72]. Accounting for the estimates of the P_{csi}^0 ($i = 1, 2, 3$) yields given before and the above-mentioned J/ψ production differential cross sections at "low" J/ψ total energies, we can evaluate the numbers of events expected in this measurement in the J/ψ energy range of 6.5–7.5 GeV for the $K^-p \rightarrow P_{csi}^0 \rightarrow J/\psi\Lambda$, $J/\psi \rightarrow e^+e^-$, $\Lambda \rightarrow p\pi^-$ reactions. They are about of 2.9–29 and 29–290 per year for $Br[P_{csi}^0 \rightarrow K^-p] = 0.001$ and 0.01%, respectively. The number of background events is lower by several orders of magnitude. This means that the observation of the hidden-charm strange pentaquarks P_{csi}^0 via the low-energy J/ψ meson production on proton target is quite optimistic at the J-PARC at least in the case when $Br[P_{csi}^0 \rightarrow K^-p] = 0.01\%$ and $Br[P_{csi}^0 \rightarrow J/\psi\Lambda] = 0.125, 0.25, 0.5$ and 1%. It should be pointed out that most likely it would be difficult to determine the spin-parity quantum numbers of the P_{csi}^0 states by using the combined total and integrated over production angles differential cross sections considered incoherently in the present work since that observables, based on the squared absolute values of the resonant and non-resonant production amplitudes, depend weakly on them. Such consideration is justified because the

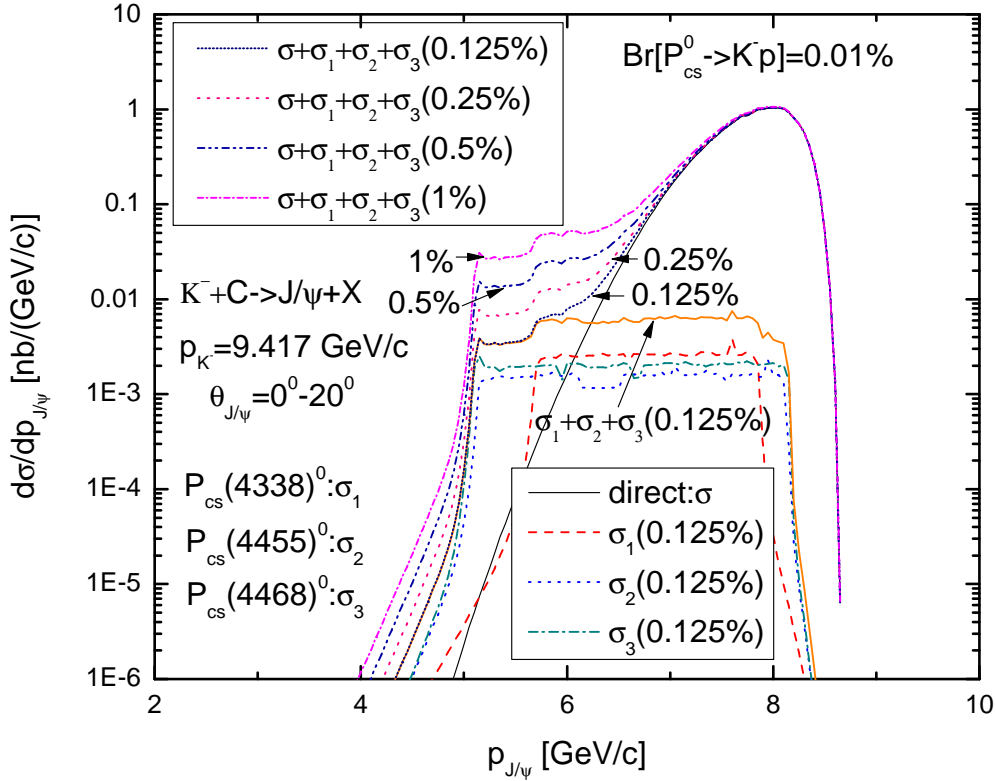


Figure 9: (Color online.) The direct non-resonant momentum distribution of J/ψ mesons, produced in the reaction $K^-^{12}\text{C} \rightarrow J/\psi X$ in the laboratory polar angular range of 0° – 20° and calculated in line with Eq. (28) at initial antikaon resonant momentum of 9.417 GeV/c in the laboratory system (black solid curve). The resonant momentum distributions of J/ψ mesons, produced in the two-step processes $K^-p \rightarrow P_{cs}(4338)^0 \rightarrow J/\psi\Lambda$, $K^-p \rightarrow P_{cs}(4455)^0 \rightarrow J/\psi\Lambda$ and $K^-p \rightarrow P_{cs}(4468)^0 \rightarrow J/\psi\Lambda$ and calculated in line with Eq. (37) at the same incident antikaon momentum of 9.417 GeV/c assuming that the resonances $P_{cs}(4338)^0$, $P_{cs}(4455)^0$ and $P_{cs}(4468)^0$ with the spin-parity assignments $J^P = (1/2)^-$, $J^P = (1/2)^-$ and $J^P = (3/2)^-$, correspondingly, all decay to the K^-p and $J/\psi\Lambda$ modes with branching fractions 0.01% and 0.125% (respectively, red dashed, blue dotted, dark cyan dashed-dotted curves) and their incoherent sum (orange solid curve). Incoherent sum of the direct non-resonant J/ψ momentum distribution and resonant ones, calculated supposing that the resonances $P_{cs}(4338)^0$, $P_{cs}(4455)^0$, $P_{cs}(4468)^0$ with the same spin-parity combinations all decay to the K^-p and $J/\psi\Lambda$ with branching fractions 0.01% and 0.125, 0.25, 0.5 and 1% (respectively, navy short-dotted, pink dotted, royal dashed-dotted-dotted and magenta short-dashed-dotted curves), all as functions of the J/ψ momentum $p_{J/\psi}$ in the laboratory frame.

role of the interference effects between resonant and non-resonant contributions in the $K^-p \rightarrow J/\psi\Lambda$ reaction as well as between different resonance states in the observables considered is expected to be insignificant due to the fact that the t -channel J/ψ production contributes only to the forward angles in the c.m. frame while the s -channel resonances contribute in a full solid angle [84]. A way of determining the P_{csi}^0 quantum numbers should be based on the model, which takes into account the interference effects via adding the resonant and non-resonant production amplitudes coherently. The results of such procedure depend, in particular, on these numbers. To probe them, another observables like angular distributions [69, 85] or polarization observables (single and double) [86,

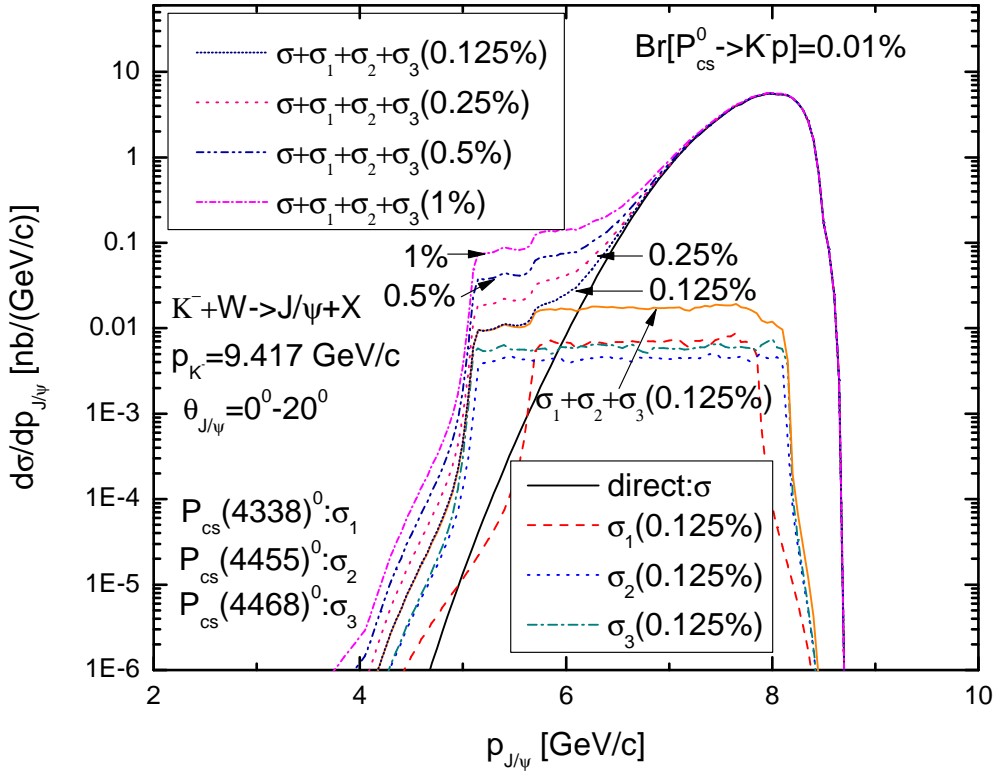


Figure 10: (Color online.) The direct non-resonant momentum distribution of J/ψ mesons, produced in the reaction $K^-^{184}\text{W} \rightarrow J/\psi X$ in the laboratory polar angular range of 0° – 20° and calculated in line with Eq. (28) at initial antikaon resonant momentum of 9.417 GeV/c in the laboratory system (black solid curve). The resonant momentum distributions of J/ψ mesons, produced in the two-step processes $K^-p \rightarrow P_{cs}(4338)^0 \rightarrow J/\psi\Lambda$, $K^-p \rightarrow P_{cs}(4455)^0 \rightarrow J/\psi\Lambda$ and $K^-p \rightarrow P_{cs}(4468)^0 \rightarrow J/\psi\Lambda$ and calculated in line with Eq. (37) at the same incident antikaon momentum of 9.417 GeV/c assuming that the resonances $P_{cs}(4338)^0$, $P_{cs}(4455)^0$ and $P_{cs}(4468)^0$ with the spin-parity assignments $J^P = (1/2)^-$, $J^P = (1/2)^-$ and $J^P = (3/2)^-$, correspondingly, all decay to the K^-p and $J/\psi\Lambda$ modes with branching fractions 0.01% and 0.125% (respectively, red dashed, blue dotted, dark cyan dashed-dotted curves) and their incoherent sum (orange solid curve). Incoherent sum of the direct non-resonant J/ψ momentum distribution and resonant ones, calculated supposing that the resonances $P_{cs}(4338)^0$, $P_{cs}(4455)^0$, $P_{cs}(4468)^0$ with the same spin-parity combinations all decay to the K^-p and $J/\psi\Lambda$ with branching fractions 0.01% and 0.125, 0.25, 0.5 and 1% (respectively, navy short-dotted, pink dotted, royal dashed-dotted-dotted and magenta short-dashed-dotted curves), all as functions of the J/ψ momentum $p_{J/\psi}$ in the laboratory frame.

87], accounting for the spin correlations between the polarized target proton and the polarized recoil J/ψ meson and Λ hyperon (spin of the incident K^- meson is equal to zero), are needed. The consideration of this aspect is beyond the scope of the present paper. One may hope that it will be studied in the future work when the appropriate K^-p data will appear to control that interference.

The momentum dependencies of the absolute non-resonant, resonant and combined J/ψ meson differential cross sections, respectively, from the direct (5), two-step (30)/(31) and direct plus two-step J/ψ production processes in $K^{-12}\text{C}$ and $K^{-184}\text{W}$ interactions, calculated on the basis of Eqs. (28), (37) for laboratory polar angles of 0° – 20° , for incident K^- meson lowest resonant momentum

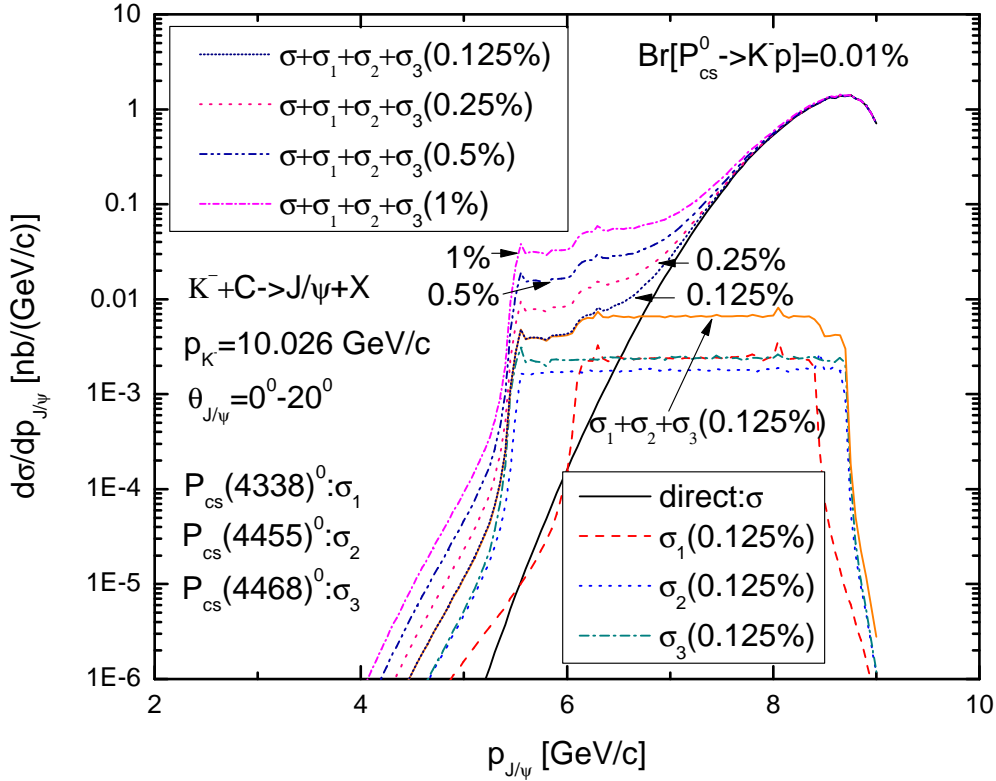


Figure 11: (Color online.) The same as in Fig. 9, but calculated for the initial antikaon momentum of 10.026 GeV/c.

of 9.417 GeV/c and for branching fractions $Br[P_{csi}^0 \rightarrow K^- p] = 0.01\%$, are shown, respectively, in Figs. 9 and 10. The same as in these figures, but determined for the initial highest antikaon resonant momentum of 10.026 GeV/c, is given in Figs. 11 and 12. And finally, the same as that shown in Fig. 12, but calculated for the three branching ratios $Br[P_{csi}^0 \rightarrow K^- p] = 0.001\%$, is presented in Fig. 13 to see the sensitivity of the combined J/ψ momentum distribution to these ratios. The resonant momentum distributions of the J/ψ mesons in the two-step processes (30)/(31), taking place on the bound protons of carbon and tungsten nuclei, were obtained for four employed values of the branching ratios $Br[P_{csi}^0 \rightarrow J/\psi \Lambda]$. It is seen from Figs. 9–12 that the total contribution to the J/ψ production on both these nuclei, stemming from all the intermediate P_{csi}^0 states, decaying to the $J/\psi \Lambda$ mode with branching fractions of 0.125% (orange solid curves), shows practically flat behavior, and it is significantly larger than that from the background process (5) (black solid curves) in the "low"-momentum regions of 4.5–6.0 GeV/c and 4.5–6.5 GeV/c for considered antikaon beam momenta of 9.417 and 10.026 GeV/c, respectively. The results, presented in Fig. 13, show that such "low"-momentum region also exists and amounts to 4.5–6.0 GeV/c for the initial K^- momentum of 10.026 GeV/c and $Br[P_{csi}^0 \rightarrow K^- p] = 0.001\%$. And in these "low"-momentum regions, what is of primary importance, the decays $P_{cs}(4455)^0 \rightarrow J/\psi \Lambda$ and $P_{cs}(4468)^0 \rightarrow J/\psi \Lambda$ are dominant. As a consequence, the combined J/ψ yield in them is practically completely governed by the presence of the $P_{cs}(4455)^0$ and $P_{cs}(4468)^0$ states in its production. For given value of the branching ratios $Br[P_{csi}^0 \rightarrow K^- p]$, the strength of the yield is almost completely determined by the branching ratios $Br[P_{cs}(4455/4468)^0 \rightarrow J/\psi \Lambda]$, used in the calculations, with a value, which, on the one hand, depends weakly on the antikaon momentum and which, on the other hand, increases by a factor

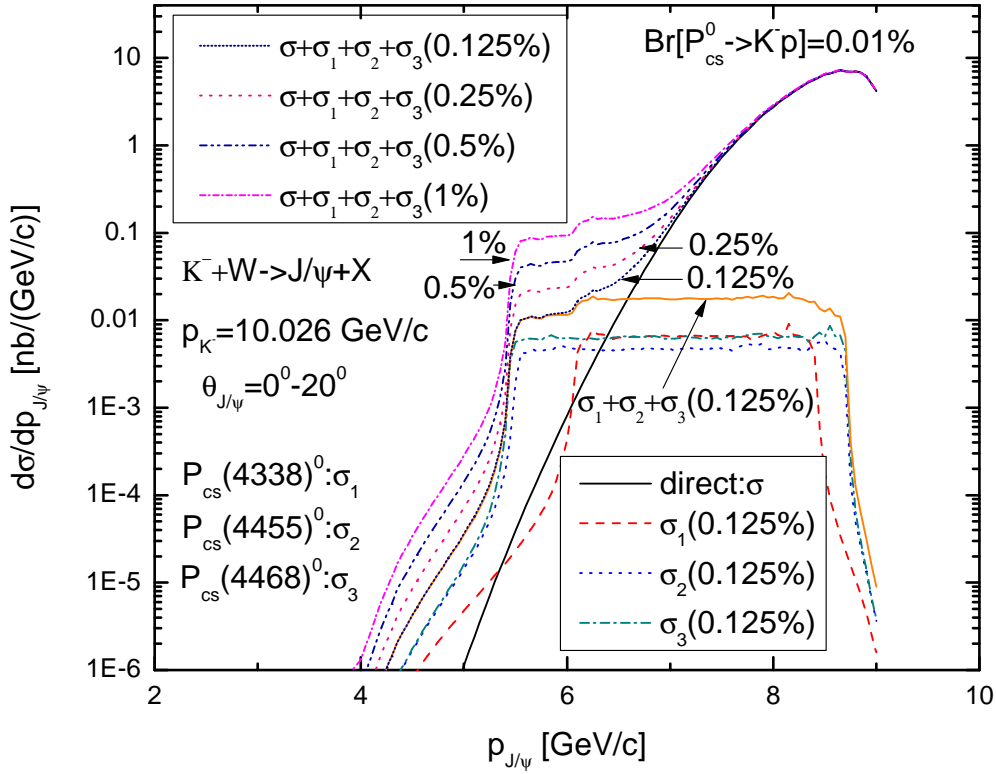


Figure 12: (Color online.) The same as in Fig. 10, but calculated for the initial antikaon momentum of 10.026 GeV/c.

of about four for both antikaon beam momenta considered, when going from carbon target nucleus to tungsten one. The value is still large enough to be measured, as one may hope, in the future experiment at the J-PARC. This results in the well separated and experimentally distinguishable differences between all combined calculations, corresponding to the employed options for these ratios, for both target nuclei, for both antikaon momenta considered and for both adopted options for the branching fractions $Br[P_{csi}^0 \rightarrow K^-p]$ ($i = 1, 2, 3$). Therefore, the J/ψ meson production differential cross section measurements on light and especially on heavy nuclear targets in the above J/ψ "low"-momentum regions at antikaon momenta in the resonance regions will open an opportunity to confirm or refute the $P_{cs}(4455)^0$ and $P_{cs}(4468)^0$ states and, if they will be confirmed, to determine their branching ratios to the $J/\psi\Lambda$ – at least to distinguish between realistic options of 0.125, 0.25, 0.5 and 1%.

Taking into account the above considerations, we can conclude that the near-threshold J/ψ energy and momentum distribution measurements in antikaon-induced reactions both on protons and on nuclear targets will provide further evidence for the existence of the hidden-charm strange pentaquark $P_{cs}(4338)^0$, for the presence of two resonances in the peak of the $J/\psi\Lambda$ mass spectrum around 4459 MeV, and will shed light on their decay rates to the channel $J/\psi\Lambda$.

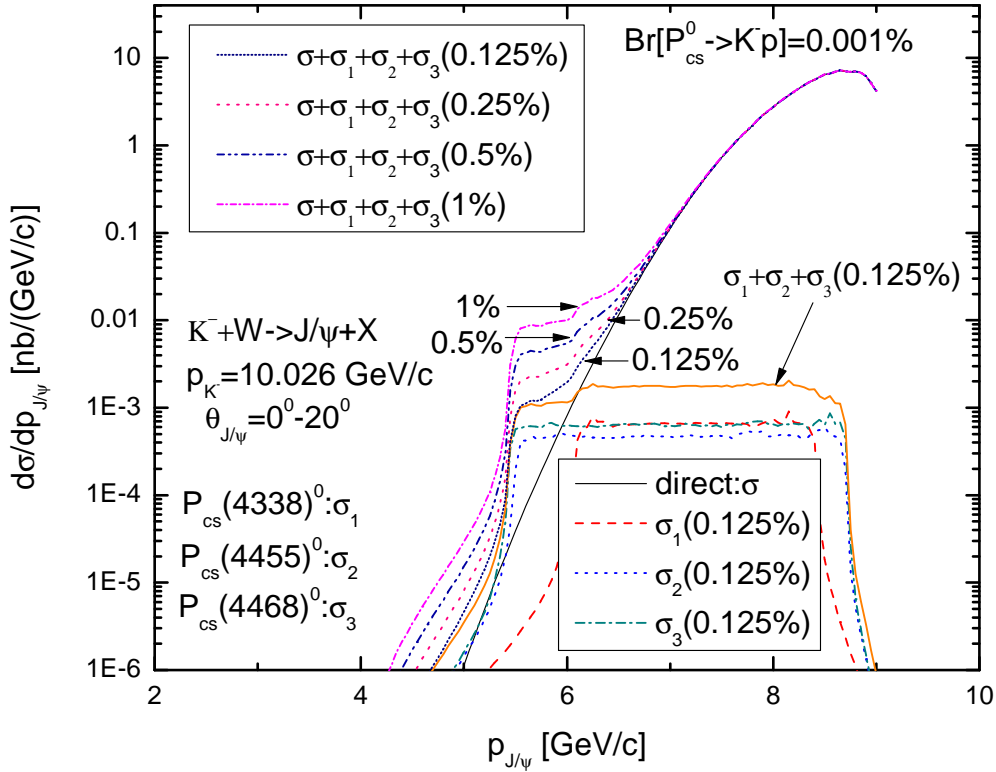


Figure 13: (Color online.) The direct non-resonant momentum distribution of J/ψ mesons, produced in the reaction $K^- + W^- \rightarrow J/\psi + X$ in the laboratory polar angular range of $0^\circ - 20^\circ$ and calculated in line with Eq. (28) at initial antikaon resonant momentum of 10.026 GeV/c in the laboratory system (black solid curve). The resonant momentum distributions of J/ψ mesons, produced in the two-step processes $K^- p \rightarrow P_{cs}(4338)^0 \rightarrow J/\psi \Lambda$, $K^- p \rightarrow P_{cs}(4455)^0 \rightarrow J/\psi \Lambda$ and $K^- p \rightarrow P_{cs}(4468)^0 \rightarrow J/\psi \Lambda$ and calculated in line with Eq. (37) at the same incident antikaon momentum of 10.026 GeV/c assuming that the resonances $P_{cs}(4338)^0$, $P_{cs}(4455)^0$ and $P_{cs}(4468)^0$ with the spin-parity assignments $J^P = (1/2)^-$, $J^P = (1/2)^-$ and $J^P = (3/2)^-$, correspondingly, all decay to the $K^- p$ and $J/\psi \Lambda$ modes with branching fractions 0.001% and 0.125% (respectively, red dashed, blue dotted, dark cyan dashed-dotted curves) and their incoherent sum (orange solid curve). Incoherent sum of the direct non-resonant J/ψ momentum distribution and resonant ones, calculated supposing that the resonances $P_{cs}(4338)^0$, $P_{cs}(4455)^0$, $P_{cs}(4468)^0$ with the same spin-parity combinations all decay to the $K^- p$ and $J/\psi \Lambda$ with branching fractions 0.001% and 0.125, 0.25, 0.5 and 1% (respectively, navy short-dotted, pink dotted, royal dashed-dotted-dotted and magenta short-dashed-dotted curves), all as functions of the J/ψ momentum $p_{J/\psi}$ in the laboratory frame.

4. Conclusions

Accounting for the LHCb observation that the reported hidden-charm strange pentaquark $P_{cs}(4459)^0$ can split into two substructures, $P_{cs}(4455)^0$ and $P_{cs}(4468)^0$, with a mass difference of 13 MeV as well as the newly observed hidden-charm pentaquark resonance $P_{cs}(4338)^0$ with strangeness, in this paper we have studied within the double-peak scenario for the $P_{cs}(4459)^0$ state the near-threshold J/ψ meson production from protons and nuclei by considering incoherent direct non-resonant ($K^- p \rightarrow J/\psi \Lambda$) and two-step resonant ($K^- p \rightarrow P_{csi}^0 \rightarrow J/\psi \Lambda$, $i = 1, 2, 3$; $P_{cs1}^0 = P_{cs}(4338)^0$),

$P_{cs2}^0 = P_{cs}(4455)^0$, $P_{cs3}^0 = P_{cs}(4468)^0$ charmonium production processes with the main goal of clarifying the possibility to observe within this scenario both above two substructures contributing to the $P_{cs}(4459)^0$ state and the $P_{cs}(4338)^0$ resonance in this production. We have calculated the absolute excitation functions, energy and momentum distributions for the non-resonant, resonant and for the combined (non-resonant plus resonant) production of J/ψ mesons on protons as well as, using the nuclear spectral function approach, on carbon and tungsten target nuclei at near-threshold incident antikaon beam momenta by assuming the spin-parity assignments of the hidden-charm resonances $P_{cs}(4338)^0$, $P_{cs}(4455)^0$ and $P_{cs}(4468)^0$ as $J^P = (1/2)^-$, $J^P = (1/2)^-$ and $J^P = (3/2)^-$ within four different realistic choices for the branching ratios of their decays to the $J/\psi\Lambda$ mode (0.125, 0.25, 0.5 and 1%) as well as for two options for the branching fraction of their decays to the K^-p channel (0.01 and 0.001%). It was shown that when the latter fraction is assumed to be 0.01% then will be very hard to measure the P_{csi}^0 pentaquark states through the scan of the J/ψ total production cross section on a proton target in the near-threshold momentum region around the resonant antikaon momenta of 9.417, 9.965 and 10.026 GeV/c if the considered branching ratios of the $J/\psi\Lambda$ decay mode $\sim 0.5\%$ and less. It was also found that if the branching fraction of the $P_{csi}^0 \rightarrow K^-p$ decays is suggested to be 0.001% then these hidden-charm pentaquark states will be not accessible in such measurements. It was further demonstrated that at these K^- meson beam momenta the J/ψ energy and momentum combined distributions of interest reveal noticeable sensitivity to all the above scenarios, respectively, at "low" J/ψ total energies and momenta, which means that they may be an important tool to provide further evidence for the existence of the strange hidden-charm pentaquark resonances $P_{cs}(4338)^0$, $P_{cs}(4455)^0$, $P_{cs}(4468)^0$ and to get valuable information on their decay rates to the K^-p initial and $J/\psi\Lambda$ final states. The measurements of these distributions could be performed in the future at the J-PARC facility. The present model's predictions can also serve as a good starting point in supporting of these measurements.

References

- [1] R. Aaij *et al.* (LHCb Collaboration), Phys. Rev. Lett. **115**, 072001 (2015); arXiv:1507.03414 [hep-ex].
- [2] T. Gershon (LHCb Collaboration), arXiv:2206.15233 [hep-ex].
- [3] R. Aaij *et al.* (LHCb Collaboration), Phys. Rev. Lett. **122**, 222001 (2019); arXiv:1904.03947 [hep-ex].
- [4] R. Aaij *et al.* (LHCb Collaboration), Phys. Rev. Lett. **128**, 062001 (2022); arXiv:2108.04720 [hep-ex].
- [5] G.-J. Wang *et al.*, Phys. Rev. D **102**, 036012 (2020); arXiv:1911.09613 [hep-ph].
- [6] F.-Z. Peng *et al.*, arXiv:2211.09154 [hep-ph].
- [7] X.-Y. Wang, X.-R. Chen, and J. He, Phys. Rev. D **99**, 114007 (2019).
- [8] H. X. Chen, W. Chen and S.-L. Zhu, Phys. Rev. D **100**, 051501 (2019); arXiv:1903.11001 [hep-ph].
- [9] R. Chen, Z. F. Sun, X. Liu and S.-L. Zhu, Phys. Rev. D **100**, 011502 (2019); arXiv:1903.11013 [hep-ph].

- [10] F. K. Guo, H. J. Jing, U. G. Meissner and S. Sakai, Phys. Rev. D **99**, 091501 (2019); arXiv:1903.11503 [hep-ph].
- [11] M. Z. Liu *et al.*, Phys. Rev. Lett. **122**, 242001 (2019); arXiv:1903.11560 [hep-ph].
- [12] J. R. Zhang, Eur. Phys. J. C **79**, 1001 (2019); arXiv:1904.10711 [hep-ph].
- [13] C. W. Xiao, J. Nieves and E. Oset, Phys. Rev. D **100**, 014021 (2019); arXiv:1904.01296 [hep-ph].
- [14] L. Meng, B. Wang, G.-J. Wang and S.-L. Zhu, Phys. Rev. D **100**, 014031 (2019); arXiv:1905.04113 [hep-ph].
- [15] T. Gutsche and V. E. Lyubovitskij, Phys. Rev. D **100**, 094031 (2019); arXiv:1910.03984 [hep-ph].
- [16] C. J. Xiao *et al.*, Phys. Rev. D **100**, 014022 (2019); arXiv:1904.00872 [hep-ph].
- [17] J. B. Cheng and Y. R. Liu, Phys. Rev. D **100**, 054002 (2019); arXiv:1905.08605 [hep-ph].
- [18] L. Meng, B. Wang, G.-J. Wang and S.-L. Zhu, arXiv:2204.08716 [hep-ph].
- [19] C.-R. Deng, Phys. Rev. D **105**, 116021 (2022); arXiv:2202.13570 [hep-ph].
- [20] Z.-G. Wang, Int. J. Mod. Phys. A **35**, 2050003 (2020); arXiv:1905.02892 [hep-ph].
- [21] M.-J. Yan *et al.*, Eur. Phys. J. C **82**, 574 (2022); arXiv:2108.05306 [hep-ph].
- [22] S. X. Nakamura, A. Hosaka and Y. Yamaguchi, Phys. Rev. D **104**, L091503 (2021); arXiv:2109.15235 [hep-ph].
- [23] X.-W. Wang and Z.-G. Wang, Chin. Phys. C **47**, 013109 (2023); arXiv:2207.06060 [hep-ph].
- [24] R. Aaij *et al.* (LHCb Collaboration), Sci. Bull. **66**,1278 (2021); arXiv:2012.10380 [hep-ex].
- [25] LHCb Collaboration, arXiv:2210.10346 [hep-ex].
- [26] M. Karliner and J. L. Rosner, Phys. Rev. D **106**, 036024 (2022); arXiv:2207.07581 [hep-ph].
- [27] F.-L. Wang and X. Liu, Phys. Lett. B **835**, 137583 (2022); arXiv:2207.10493 [hep-ph].
- [28] M. Z. Liu, Y. W. Pan and L. S. Geng, Phys. Rev. D **103**, 034003 (2021); arXiv:2011.07935 [hep-ph].

- [29] L. Meng, B. Wang and S.-L. Zhu, Phys. Rev. D **107**, 014005 (2023); arXiv:2208.03883 [hep-ph].
- [30] P. G. Ortega, D. R. Entem and F. Fernandez, Phys. Lett. B **838**, 137747 (2023); arXiv:2210.04465 [hep-ph].
- [31] J.-T. Zhu, S.-Y. Kong and J. He, Phys. Rev. D **107**, 034029 (2023); arXiv:2211.06232 [hep-ph].
- [32] K. Chen, Z.-Y. Lin and S.-L. Zhu, arXiv:2211.05558 [hep-ph].
- [33] Z.-Y. Yang *et al.*, arXiv:2211.08211 [hep-ph].
- [34] F. Yang, Y. Huang and H. Q. Zhu, Sci. China-Phys. Mech. Astron. **64**, 121011 (2021); arXiv:2107.13267 [hep-ph].
- [35] X. Hu and J. Ping, Eur. Phys. J. C **82**, 118 (2022); arXiv:2109.09972 [hep-ph].
- [36] H. X. Chen, W. Chen, X. Liu, and X. H. Liu, Eur. Phys. J. C **81**, 409 (2021); arXiv:2011.01079 [hep-ph].
- [37] C. W. Xiao, J. J. Wu and B. S. Zou, Phys. Rev. D **103**, 054016 (2021); arXiv:2102.02607 [hep-ph].
- [38] M.-L. Du, Z.-H. Guo and J. A. Oller, Phys. Rev. D **104**, 114034 (2021); arXiv:2109.14237 [hep-ph].
- [39] Z.-G. Wang, Int. J. Mod. Phys. A **36**, 2150071 (2021); arXiv:2011.05102 [hep-ph].
- [40] K. Azizi, Y. Sarac, and H. Sundu, Phys. Rev. D **103**, 094033 (2021); arXiv:2101.07850 [hep-ph].
- [41] P.-P. Shi, F. Huang and W.-L. Wang, Eur. Phys. J. A **57**, 237 (2021); arXiv:2107.08680 [hep-ph].
- [42] E. Santopinto and A. Giachino, Phys. Rev. D **96**, 014014 (2017); arXiv:1604.03769 [hep-ph].
- [43] A. Feijoo, W.-F. Wang, C.-W. Xiao, J. J. Wu, E. Oset, J. Nieves and B. -S. Zou, Phys. Lett. B **839**, 137760 (2023); arXiv:2212.12223 [hep-ph].
- [44] J. J. Wu, R. Molina, E. Oset and B. S. Zou, Phys. Rev. Lett. **105**, 232001 (2010); arXiv:1007.0573 [nucl-th].
- [45] J. J. Wu, R. Molina, E. Oset and B. S. Zou, Phys. Rev. C **84**, 015202 (2011); arXiv:1011.2399 [nucl-th].
- [46] Z. G. Wang, Eur. Phys. J. C **76**, 142 (2016); arXiv:1509.06436 [hep-ph].
- [47] R. Chen, J. He and X. Liu, Chin. Phys. C **41**, 103105 (2017); arXiv:1609.03235 [hep-ph].

- [48] C. W. Xiao, J. Nieves, and E. Oset, Phys. Lett. B **799**, 135051 (2019); arXiv:1906.09010 [hep-ph].
- [49] A. Ali *et al.*, JHEP **2019**, 256 (2019); arXiv:1907.06507 [hep-ph].
- [50] B. Wang, L. Meng and S.-L. Zhu, Phys. Rev. D **101**, 034018 (2020); arXiv:1912.12592 [hep-ph].
- [51] H. X. Chen, L. S. Geng, W. H. Liang *et al.*, Phys. Rev. C **93**, 065203 (2016); arXiv:1510.01803 [hep-ph].
- [52] A. Feijoo, V. K. Magas, A. Ramos and E. Oset, Eur. Phys. J. C **76**, 446 (2016); arXiv:1512.08152 [hep-ph].
- [53] J. X. Lu, E. Wang, J. J. Xie, L. S. Geng and E. Oset, Phys. Rev. D **93**, 094009 (2016); arXiv:1601.00075 [hep-ph].
- [54] R. Chen, Phys. Rev. D **103**, 054007 (2021); [arXiv:2011.07214 [hep-ph]]; R. Chen, Eur. Phys. J. C **81**, 122 (2021) [arXiv:2101.10614 [hep-ph]].
- [55] F. Z. Peng, M. J. Yan, M. Sanchez Sanchez, and M. P. Valderrama, Eur. Phys. J. C **81**, 666 (2021); arXiv:2011.01915 [hep-ph].
- [56] J.-T. Zhu, L.-Q. Song and J. He, Phys. Rev. D **103**, 074007 (2021); arXiv:2101.12441 [hep-ph].
- [57] M. Ablikim *et al.* (BESIII Collaboration), Phys. Rev. Lett. **126**, 102001 (2021); arXiv:2011.07855 [hep-ex].
- [58] L. Meng, B. Wang and S.-L. Zhu, Phys. Rev. D **102**, 111502 (2020); arXiv:2011.08656 [hep-ph].
- [59] Z. Yang *et al.*, Phys. Rev. D **103**, 074029 (2021); arXiv:2011.08725 [hep-ph].
- [60] M. Ablikim *et al.* (BESIII Collaboration), Phys. Rev. Lett. **129**, 112003 (2022); arXiv:2204.13703 [hep-ex].
- [61] R. Aaij *et al.* (LHCb Collaboration), Phys. Rev. Lett. **127**, 082001 (2021); arXiv:2103.01803 [hep-ex].
- [62] M. Ablikim *et al.* (BESIII Collaboration), Chin. Phys. C **47**, 033001 (2023); arXiv:2211.12060 [hep-ex].
- [63] F. L. Wang, R. Chen and X. Liu, Phys. Rev. D **103**, 034014 (2021);
- [64] F. L. Wang, X. D. Yang, R. Chen and X. Liu, Phys. Rev. D **103**, 054025 (2021); arXiv:2101.11200 [hep-ph].
- [65] K. Azizi, Y. Sarac and H. Sundu, Eur. Phys. J. C **82**, 543 (2022); arXiv:2112.15543 [hep-ph].

- [66] K. Azizi, Y. Sarac and H. Sundu, Phys. Rev. D **107**, 014023 (2023);
arXiv:2210.03471 [hep-ph].
J. A. Marse-Valera, V. K. Magas and A. Ramos, Phys. Rev. Lett. **130**, 091903 (2023);
arXiv:2210.02792 [hep-ph].
- [67] U. Ozdem, arXiv:2303.10649 [hep-ph].
U. Ozdem, Phys. Lett. B **836**, 137635 (2023); arXiv:2208.07684 [hep-ph].
U. Ozdem, Eur. Phys. J. C **81**, 277 (2021); arXiv:2102.01996 [hep-ph].
- [68] H.-X. Chen, W. Chen, X. Liu, Y.-R. Liu and S.-L. Zhu, Rept. Prog. Phys. **86**, 026201 (2023);
arXiv:2204.02649 [hep-ph].
- [69] S. Clymton, H.-J. Kim and H.-C. Kim, Phys. Rev. D **104**, 014023 (2021);
arXiv:2102.08737 [hep-ph].
- [70] E. Ya. Paryev, Nucl. Phys. A **1023**, 122452 (2022);
arXiv:2205.00728 [hep-ph].
- [71] C. Cheng, F. Yang and Y. Huang, Phys. Rev. D **104**, 116007 (2021);
arXiv:2110.04746 [hep-ph].
- [72] H. Ohnishi, F. Sakuma, T. Takahashi, Prog. Part. Nucl. Phys. **113**, 103773 (2020);
arXiv:1912.02380 [nucl-ex].
K. Aoki *et al.*, arXiv:2110.04462 [nucl-ex].
- [73] P.-P. Shi, F.-K. Guo and Z. Yang, Phys. Rev. D **106**, 114026 (2022);
arXiv:2208.02639 [hep-ph].
- [74] C. Gobbi, C. B. Dover and A. Gal, Phys. Rev. C **50**, 1594 (1994).
- [75] S. X. Nakamura and J. J. Wu, arXiv:2208.11995 [hep-ph].
- [76] A. Ali *et al.* (The GlueX Collaboration), Phys. Rev. Lett. **123**, 072001 (2019);
arXiv:1905.10811 [nucl-ex].
- [77] S. Joosten. Quarkonium production near threshold at JLab and EIC,
9th Workshop of the APS Topical Group on hadron physics (2021).
URL <https://indico.jlab.org/event/412/contributions/8266/attachments/6888/9385/20210416-GHP-Jpsi-Threshold.pdf>
- [78] E. Ya. Paryev, Nucl. Phys. A **1029**, 122562 (2023);
arXiv:2211.16037 [hep-ph].
- [79] X. Cao, J.-P. Dai, Phys. Rev. D **100**, 054033 (2019);
arXiv:1904.06015 [hep-ph].
- [80] X.-Y. Wang, J. He, X.-R. Chen, Q. Wang, and X. Zhu, Phys. Lett. B **797**, 134862 (2019);
arXiv:1906.04044 [hep-ph].
- [81] Q. Wang, X.-H. Liu and Q. Zhao, Phys. Rev. D **92**, 034022 (2015);
arXiv:1508.00339 [hep-ph].
- [82] J. J. Wu, T.-S.H. Lee and B. S. Zou, Phys. Rev. C **100**, 035206 (2019);
arXiv:1906.05375 [nucl-th].

- [83] Y. Huang *et al.*, J. Phys. G, Nucl. Part. Phys. **41**, 115004 (2014);
arXiv:1305.4434 [nucl-th].
- [84] X. Cao *et al.*, Phys. Rev. D **101**, 074010 (2020);
arXiv:1912.12054 [hep-ph].
- [85] B. G. Yu, T. K. Choi and C.-R. Ji, Phys. Rev. C **70**, 045205 (2004);
arXiv:nucl-th/0312075.
- [86] B. G. Yu, T. K. Choi and C.-R. Ji, J. Phys. G **32**, 387 (2006);
arXiv:nucl-th/0408006.
- [87] D. Winney *et al.*, Phys. Rev. D **100**, 034019 (2019);
arXiv:1907.09393 [hep-ph].